Spin polarization and magnetic dichroism in photoemission from core and valence states in localized magnetic systems. III. Angular distributions

B. T. Thole
Material Science Center, University of Groningen, 9747 AG Groningen, The Netherlands

Gerrit van der Laan
Daresbury Laboratory, Warrington WA4 4AD, United Kingdom
(Received 2 September 1993)

A general analysis is presented for angle-dependent photoemission from magnetic and oriented atoms using linearly and circularly polarized x-rays. The anisotropy in the angular distribution in a localized material is due to the polarization of the photon, the polarization of the shell from which the electron is emitted, and the Coulomb and exchange interactions of the hole with the polarized valence electrons in the final state of the photoionized atom. The angular dependence of the dipole excited photoemission gives the same information about the multipole orbital and spin magnetic moments of the atom as excitation with quadrupole or octupole radiation. It is shown that the photoemission spectrum at an arbitrary angle is a linear combination of the fundamental spectra, which contain all the physical information of the atom. Redundancy in the measurements makes it possible to obtain these fundamental spectra in completely different ways, allowing to choose the most advantageous geometry and polarization, e.g., the magnetic circular dichroism can be also be measured with linear polarization. Circular dichroism in the angular dependence, magnetic linear dichroism in the angular dependence, and spin polarization are treated using the same analysis. We explain the strong angle dependence observed in the rare-earth $5p$ photoemission, in the circular dichroism of the $3d$ transition-metal $2p$ core-level photoemission and the rare-earth $4f$ photoemission.

I. INTRODUCTION

Natural circular dichroism in optical spectroscopy arises from an interference between electric and magnetic dipole transitions. The magneto-optical Kerr effect, Faraday effect, and the recently discovered magnetic x-ray dichroism[1] are caused by electric dipole transitions from a magnetic polarized ground state with spin-orbit interaction. The advent of intense sources of synchrotron radiation with a high degree of polarization now makes it possible to study circular dichroism in photoemission. The presence of dichroism in the excitation of an electron from a core level to a free-electron continuum level requires an electrostatic interaction between the core and the valence state.[2] This interaction gives a final-state multiplet structure, where each individual level has a specific polarization dependence given by the alignment, in that state, of the angular momenta of the created core hole and the valence shell.[3,4] This polarization dependence can be used to disentangle the satellite structure and multiplet structure, which are often simultaneously present in the photoelectron spectra of correlated materials, such as transition-metal and rare-earth compounds. This paper describes a method to obtain the maximum amount of information from the angle-dependent photoemission.

The study of the angular dependence in photoionization and (in the case of negative ions) photo detachment in atomic and molecular physics has a long history. For nonoriented systems, Yang[5] already showed that the asymmetry parameter in conjunction with the partial cross section gives a complete description for the dipole excited photoemission. These two parameters can be used to study the configuration interaction and vibration modes of the photo excited state. The theory of the photoelectron angular distributions for hydrogenic atoms has been given by Bethe and Salpeter[6] and was further developed by Cooper and Zare[7] for nonhydrogenic central potentials. Jacobs[8] and later Klar and Kleinpoppen[9] obtained expressions for the angular distributions and polarization of photoelectrons for an arbitrary atomic system in terms of the density matrix, using the spherical tensor operator formalism,[10] which was developed in nuclear physics to describe the phenomenon of angular correlation of γ rays emitted in cascade transitions.[11] A theory developed by Fano and Dill,[12] which expanded the photoionization amplitude into alternative transfers of angular momentum from the photon to the electron, has been extensively used in collision dynamics, photofragmentation, and molecular photodissociation. Klar[13] extended this formalism to the spin polarization of the photoelectrons. The angular dependence in the regions around resonances was treated by Kabachnik and Sazhina[14] and by Dill.[15]

The phenomenon of circular dichroism in the angular distribution (CDAD) was predicted by Ritchie[16] in nonchiral, but oriented, molecules in a collinear measurement with the detection along the molecular axis. The effect was small because it required an interference between electric and magnetic dipole transitions. A much larger effect was predicted by Cerepkov[17] within the electric dipole approximation for oriented nonchiral mole-

 ©1994 The American Physical Society

cules in a special geometry. The direction of the emitted electron gives an additional vector in space, which can make the experimental geometry chiral. When the light polarization vector, the Z axis of the system (e.g., the molecular axis) and the emission direction of the photoelectron, are not coplanar, the geometries with left- and right-circularly polarized light are no longer mirror images. Then the interference term between the $l+1$ and $l-1$ photoemission channels gives CDAD with a magnitude that depends on the radial matrix elements and the phase difference of these channels. A numerical calculation for the 4σ orbital of an oriented CO molecule by Dubs, Dixit, and McKoy[18] shows a pronounced effect with maxima of almost 100% asymmetry. Spin-dependent interactions and spin-orbit interaction are not required and this effect can be observed in adsorbates on metal surfaces,[19] systems prepared by photon[20] and particle impact,[21] and external fields and photofragmentation.[22–25] These methods give systems with aligned or oriented moments similar to that in (anti)ferromagnetic materials, where the moments are polarized by magnetic interactions producing long-range order. Thus, circular polarization can be used when the time-reversal symmetry of the orbits is broken, such as in magnetic materials with spin-orbit interaction and nonmagnetic materials with chiral symmetry or in a chiral geometry. A linear analog of CDAD was recently reported by Roth *et al.*[26] at the Fe $3p$ level of ferromagnetic iron.

The spin direction measurement can also make the geometry chiral. Lee[27] predicted an angular distribution in the spin polarization from unpolarized atoms excited with unpolarized light. The influence of the spin is indirect because the electric dipole operator acts only on the orbital. Because the spin of the emitted electron is the same as the spin of the core hole, the photoelectron spin is polarized when the core electron spin is polarized which can be induced both by electrostatic interactions with the valence shell or by spin-orbit interaction with its own orbit.

Magnetic circular dichroism in core-level photoemission was reported by Baumgarten *et al.*[28] This technique has the advantage over spin-resolved photoemission that it does not require a spin detector, which has a low efficiency. In papers I (Ref. 3) and II (Ref. 4) we presented a general analysis of circular dichroism and spin polarization in angle-integrated photoemission from closed and open shells, respectively. With the use of many-particle theory, general equations were derived for the six fundamental spectra which are special linear combinations of the spin-polarized photoemission spectra measured with left-, Z, and right-circularly polarized radiation. These fundamental spectra, which are the isotropic spectrum, spin spectrum, magnetic circular dichroism, spin-orbit spectrum, anisotropic spectrum, and anisotropic spin spectrum give the correlation between the spin, orbital, and quadrupole momenta in the ground state and the spin and orbit of the hole created after photoemission.[3] For emission from an incompletely filled shell the integrated intensities of the fundamental spectra are proportional to the expectation values of the number of electrons, spin magnetic moment, orbital magnetic moment, the alignment between orbital and spin magnetic moment, the quadrupole moment, and the correlation between quadrupole and spin magnetic moment, respectively.[4]

Recently, Schneider, and co-workers[29,30] observed a strong angular dependence in the magnetic circular dichroism of the $2p$ photoemission from ferromagnetic iron. Using a one-electron picture they showed that the circular dichroism of the $2p_{1/2}$ core level is composed of an isotropic term, which depends on the relative orientation of the incident light and the magnetization, and an angular-dependent term which depends on the relative orientation of the incident light and the magnetization direction with respect to the detection direction. In this paper we will extend the analysis given in paper I and II to the angle dependence of the photoelectron and the photon. We will show that the angular distribution measures higher poles than the angle-integrated photoemission. By selecting specific emission angles we can obtain the same information about these higher moments as by using multipole radiation. The angular distribution in a localized material is due to the polarization of the photon, the polarization of the shell from which the electron is emitted, and the Coulomb and exchange interactions of the hole with the polarized valence electrons in the final state of the photoionized atom.

We will assume a continuum state which has only interactions with the emitting atom, thus we neglect angular structure induced by the nonspherical potential of the molecule or lattice. We will also not consider the loss of "memory" of the excitation process by the emitted electron due to scattering in the solid or due to refraction at the surface. The scattering of the photoelectron by the nonspherical environment can be used to study the symmetry of the atomic site, such as in photoelectron diffraction[31,32] and photoelectron holography.[33,34] In spin-polarized photoemission the scattering lengths of photoelectrons with spin up and down may be different depending on the filling of the majority and minority spin bands. The main aim of this paper is to show that all information is contained in the fundamental spectra, and we give only a short discussion of special effects due to the structure of the continuum wave function.

The outline of this paper is as follows. The theory of the angle dependence without spin detection is given in Sec. II, and the extension to spin polarization is given separately in Sec. III. Section IV discusses the effects of a nonspherical environment. The interpretation of the fundamental spectra is discussed in Sec. V. The influence of the symmetry of the atom is treated in Sec. VI, and the analysis of the angular distributions in Sec. VII. Several recent measurements are analyzed in Sec. VIII and conclusions are given in Sec. IX. The appendix gives some technical information on the necessary angular algebra.

II. SPIN-INTEGRATED THEORY

A. Recoupling the moments

Consider an atom in a ground state $\langle g|$. Applying radiation we assume that there is a part of the spectrum

which can be considered as arising from the process of taking an electron from a shell with orbital momentum l and putting it into a continuum state with orbital momentum c. In the dipole approximation c can be $l+1$ and $l-1$, and there can be interference between these channels. In order to remain more general we will consider Q-pole radiation where c can be $l+Q \cdots l-Q$ with $l+Q+c$ even. The probability of detecting the emitted electron in the direction ε (a unit vector) leaving the atom in the final state $|f\rangle$ is then [c.f. Eqs. (A1) and (A2)]

$$|D_{qq'}(\varepsilon)|^2=\sum_{\sigma m m'\gamma\gamma' cc'}\langle g|l^{\dagger}_{m\sigma}|f\rangle\langle f|l_{m'\sigma}|g\rangle(-1)^{2l-m+m'}\begin{pmatrix} l & Q & c\\ -m & q & \gamma\end{pmatrix}\begin{pmatrix} l & Q' & c'\\ -m' & q' & \gamma'\end{pmatrix}Y^{c}_{\gamma}(\varepsilon)Y^{c'}_{\gamma'}(\varepsilon)^*$$

$$=\sum_{\sigma m m' cc'}\langle g|l^{\dagger}_{m\sigma}|f\rangle\langle f|l_{m'\sigma}|g\rangle$$

, (1)

where $l^{\dagger}_{m\sigma}$ and $l_{m\sigma}$ denote the creation and annihilation operators for an l shell electron with orbital component m and spin component σ. The $Y^{c}_{\gamma}(\varepsilon)$ are spherical harmonics, which in the graphical representation[35] of the 3-j symbols are represented by the dotted lines [c.f. Eq. (A3)]. Introduction of l and l' would describe the case of hybridized valence shells or molecules. Our formulas can be easily extended to these cases but we will only treat the more highly symmetric case $l=l'$ here. The interference between the $Q+1$ final-state channels c and c' with their orbital components γ and γ' is taken into account. We will not study here the interference between different multipoles of the radiation, thus we will take $Q'=Q$. The components of the polarization of the light are $q=-Q \cdots +Q$, for dipole radiation $q=-1,0,+1$ denote right-circularly, Z-linearly, and left-circularly polarized radiation, respectively. For generality we introduce both q and q', which are required in Eq. (6) for the dependence on the direction of the light, when it is not along the Z axis. Except for this, Eq. (1) is sufficient to calculate the whole spectrum in any geometry but the main aim of this paper is to recouple it to show the symmetry aspects more clearly:

$$|D_{qq'}(\varepsilon)|^2=\sum_{x\xi\sigma m m' cc'}\langle g|l^{\dagger}_{m\sigma}|f\rangle\langle f|l_{m'\sigma}|g\rangle(-1)^{l-m}\begin{pmatrix} l & x & l\\ -m & \xi & m'\end{pmatrix}\sum_{ab}[abx]\begin{Bmatrix} l & x & l\\ c & b & c'\\ Q & a & Q\end{Bmatrix}$$

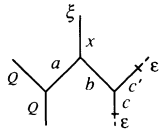

, (2)

where we applied the theorems of Yutsis, Levinson, and Vanagas[35–37] [see Eqs. (A14)–(A16)] introducing sums over the auxiliary quantum numbers a, b, and x of the photon, photoelectron, and atom, respectively. $[abx]$ is shorthand for $(2a+1)(2b+1)(2x+1)$.

B. Fundamental spectra

It is now possible to separate the physical properties of the atom from the part describing the geometry of the experiment. The physical properties are what we are interested in and the geometry is something that has to be chosen in an optimal way to measure them. The physical properties are the spectra I^{x}_{ξ} defined as

$$I^{x}_{\xi}\equiv n^{-1}_{lx}\sum_{\sigma m m'}\langle g|l^{\dagger}_{m\sigma}|f\rangle\langle f|l_{m'\sigma}|g\rangle \times(-1)^{l-m}\begin{pmatrix} l & x & l\\ -m & \xi & m'\end{pmatrix}, \quad (3)$$

where we used the normalization factor n_{lx} to remove square roots from quantities we define [Eq. (A7)]. Here, as in the following, these factors have been chosen such as to produce neatly normalized quantities. For example, the I^{x}_{ξ} spectra are of the same order of magnitude for different x. This can be understood when we observe in Eq. (3) that the 3-j symbol divided by the factor n_{lx} gives 1 for $m=m'=l$ for each value of x. The interpretation of the spectra is discussed in Sec. V.

C. Angle dependence

The angle-dependent factor in Eq. (2) giving the dependence on the polarization of the light and on ε is

$$U^{Qabx}_{qq'\xi}(\varepsilon)\equiv$$

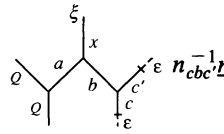

$$n^{-1}_{cbc'}\underline{n}^{-1}_{abx}4\pi[cc']^{1/2}$$

$$=$$

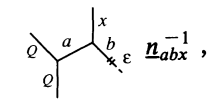

$$\underline{n}^{-1}_{abx}, \quad (4)$$

where the dotted line with double cross bar denotes the normalized spherical harmonic

$$C^{k}_{\kappa}(\theta,\varphi)=\left[\frac{4\pi}{2k+1}\right]^{1/2}Y^{k}_{\kappa}(\theta,\varphi),$$

$\underline{n}$ is defined such as to give a neat normalization of the angle dependence, see Eq. (A9). Note that the result does not depend on cc' anymore.

Terms with different a can be separated by changing the polarization of the light. For this we will define special linear combinations of the U factors and explain how these can be measured.

Defining the coefficients

TABLE I. The values of $r^{1a}_{qq'}(\mathbf{Z})$ [Eq. (7)] which give the coefficients for right-circularly, linearly, and left-circularly polarized dipole radiation along **Z** for measurement of the $a=0$, 1 and 2 spectra.

$a\backslash q$	-1	0	1
0	1	1	1
1	-1	0	1
2	1	-2	1

$$r^{Qa}_{qq'}(\mathbf{P}) \equiv n^{-1}_{Qa}$$

$$= \sum_{\alpha} n^{-1}_{Qa} C^{a}_{\alpha}(\mathbf{P})(-1)^{Q-q} \begin{pmatrix} Q & a & Q \\ -q & \alpha & q' \end{pmatrix}, \quad (5)$$

we can take the following linear combinations of intensities:

$$J^{Qa}(\mathbf{P},\varepsilon) = \sum_{qq'} r^{Qa}_{qq'}(\mathbf{P}) |D_{qq'}(\varepsilon)|^2 . \quad (6)$$

The interpretation of the particular linear combinations of spectra chosen in Eq. (6) can be found by rotating the coordinate system such that the Z axis is along the vector **P**. Then because $C^{a}_{\alpha}(\mathbf{Z})$ is nonzero only for $\alpha=0$, forcing $q=q'$, we have for the coefficients

$$r^{Qa}_{qq'}(\mathbf{P}) = \delta_{qq'} n^{-1}_{Qa}(-1)^{Q-q} \begin{pmatrix} Q & a & Q \\ -q & 0 & q' \end{pmatrix}, \quad (7)$$

which for dipole transitions ($Q=1$) are given in Table I. We see that for $a=0$ we add $q=-1,0$, and 1 and so measure the isotropic spectrum. For $a=1$ we subtract the spectra for $q=1$ and -1, i.e., left- and right-circularly polarized light propagating along **P** and so measure circular dichroism. For $a=2$ we measure the linear dichroism, subtracting the intensity for light polarized perpendicular ($q=1$ and -1) and parallel ($q=0$) to **P**. The coefficients for quadrupole ($Q=2$) and octupole ($Q=3$) transitions are given in Tables II and III. The angle-dependent factor in $J^{Qa}(\mathbf{P},\varepsilon)$ now is

$$U^{abx}_{\xi}(\mathbf{P},\varepsilon) \equiv \sum_{qq'a'} n^{-1}_{Qa}$$

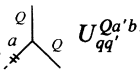

$$U^{Qa'bx}_{qq'\xi}(\varepsilon)$$

$$= \sum_{\alpha\beta} \underline{n}^{-1}_{abx} \begin{pmatrix} a & b & x \\ -\alpha & -\beta & \xi \end{pmatrix} C^{a}_{\alpha}(\mathbf{P}) C^{b}_{\beta}(\varepsilon) . \quad (8)$$

These functions are the "bipolar spherical harmonics"[38] normalized such that when ε and **P** are along the **Z** axis we have $U^{abx}_{\xi}(\mathbf{Z},\mathbf{Z})=\delta_{\xi 0}$. They are quite complicated functions of the angles defining the mutual directions of **P**, ε, and the **Z** axis except for small values of a, b, and x. However their calculation is straightforward and can be considered a trivial part of the problem. For $\xi=0$ their values are equal to the functions $U^{abx}(\mathbf{P},\varepsilon,\mathbf{Z})$, some of which are given in Sec. VIII (Table IX).

D. Total intensity

Finally Eq. (1) has to be multiplied by the reduced dipole matrix elements and the phases of the outgoing waves

$$\langle l\|C^{Q}\|c\rangle\langle c'\|C^{Q}\|l\rangle e^{i(\delta_c-\delta_{c'})} = [l][cc']^{1/2} n_{lQc} n_{lQc'} R^{lQc} R^{lQc'} e^{i(\delta_c-\delta_{c'})} , \quad (9)$$

where δ_c is the phase shift of the c wave and R are the radial matrix elements. Defining the numerical factors

$$A^{Qcc'l}_{abx} \equiv (-1)^{Q+l+x}[lcc'bx] n_{lx} \underline{n}_{abx} n^{-1}_{Qa} \times n_{cbc'} n_{lQc} n_{lQc'} \begin{Bmatrix} l & x & l \\ c & b & c' \\ Q & a & Q \end{Bmatrix}, \quad (10)$$

which are independent of ξ, [see also Eq. (A13)] we obtain for the total emission intensity in direction ε for the light polarization specified by a and **P**

$$J^{Qa}(\mathbf{P},\varepsilon) = \frac{1}{4\pi} \sum_{x\xi} I^{x}_{\xi} \sum_{b} U^{abx}_{\xi}(\mathbf{P},\varepsilon) B^{Ql}_{abx} , \quad (11)$$

where

$$B^{Ql}_{abx} = \sum_{cc'} A^{Qcc'l}_{abx} R^{lQc} R^{lQc'*} e^{i(\delta_c-\delta_{c'})} . \quad (12)$$

When $a+b+x$ is even the A factor is symmetric in c and c' and so the phase shift factor gives $2\cos(\delta_c-\delta_{c'})$. When $a+b+x$ is odd, A is imaginary and antisymmetric in c and c' and so we obtain a factor $2\sin(\delta_c-\delta_{c'})$.

From Eq. (11), which is our main result, the factors governing the angle dependence are immediately clear. The expression for the angular-dependent photoemission is a sum of terms containing energy-dependent factors (i.e., spectra) I, which are the fundamental spectra introduced in paper I and which contain all the physical information about the many-electron system that can be measured in these experiments. The angular distribution is

TABLE II. The values of $r^{2a}_{qq'}(\mathbf{Z})$ [Eq. (7)] which give the coefficients for q-polarized quadrupole radiation along **Z** for measurement of the a spectra.

$a\backslash q$	-2	-1	0	1	2
0	1	1	1	1	1
1	-1	$-1/2$	0	1/2	1
2	1	$-1/2$	-1	$-1/2$	1
3	-1	2	0	-2	1
4	1	-4	6	-4	1

TABLE III. The values of $r^{3a}_{qq'}(\mathbf{Z})$ [Eq. (7)] which give the coefficients for q-polarized octupole radiation along **Z** for measurement of the a spectra.

$a \backslash q$	−3	−2	−1	0	1	2	3
0	1	1	1	1	1	1	1
1	−1	−2/3	−1/3	0	1/3	2/3	1
2	1	0	−3/5	−4/5	−3/5	0	1
3	−1	1	1	0	−1	−1	1
4	1	−7/3	1/3	2	1/3	−7/3	1
5	−1	4	−5	0	5	−4	1
6	1	−6	15	−20	15	−6	1

essentially derived in a one-electron calculation since the photon polarization and the angle distribution act on the same electron.

Each I produces a limited set of angular distributions U with coefficients B containing contributions from each channel as a numerical factor A times the radial matrix elements R and phase shifts.

Each spectrum I^x_ξ contains the probabilities of reaching the final states of the atom by annihilation of electrons of kinds specified by x and ξ. So if, e.g., we go to a final state with a high L value this means that core hole (and thus photoelectron) and valence shell have their orbital moments parallel in this particular final state and if the valence shell is polarized then so is the core hole and this will show up in I^1_0.

Figure 1 gives a schematic picture of the angular dependence U as is given in Eq. (8). The three polarizations which appear in the photoemission process are given in the circles. The light polarization **P**, the photoelectron direction ε, and the atomic shell multipoles with respect to the **Z** axis have moments a, b, and x, respectively. The moments $a=0$, 1, and 2 represent isotropic, circular, and linear light. The moment of the angular distribution b is even because the shell l has a definite parity; $b=0$ represents the isotropic distribution. Odd x values denote oriented magnetic moments and even values denote aligned moments.

The 3-j symbol imposes the condition $|a-b| \le x \le a+b$. Because of parity $a+x$ must be even for an in-plane geometry but can be odd in an out-of-plane geometry giving CDAD and magnetic linear dichroism in the angular dependence (MLDAD), where x is odd and even and a is even and odd, respectively. This is discussed in more detail in Sec. VII.

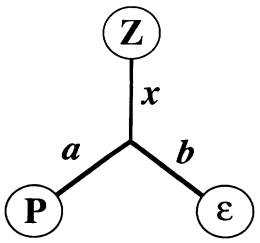

FIG. 1. Schematic picture of the angular dependence. The light polarization **P**, the photoelectron direction ε and the atomic shell multipoles with respect to the **Z** axis have moments a, b, and x respectively.

E. Measurements

It has been our aim to define the I^x_ξ in such a way that we may expect them to be generally of the same order of magnitude for all x and ξ typically consisting of a set of peaks with an (integrated) intensity of the order of unity each, but of different signs, except that the isotropic spectrum I^0 has all peaks positive and integrates to the number of l electrons. Further the U^{abx} also have comparable magnitudes. For example, for $a+b+x$ is even and $\xi=0$ their maximum value is 1 for **P** and ε along the Z axis and except for U^{000} these functions have nodes and so their range is between 1 and 2. Therefore, within each "channel" (c,c') we can immediately see from the value of the $A^{Qcc'l}_{abx}$ involved, which spectrum x and which kind of light polarization a gives an important contribution to the angle dependence. The ease of detection of a combination abx will generally be determined by its intensity compared to the isotropic signal $a=b=x=0$, where we have

$$A^{Qccl}_{000}=[c]n^2_{lQc}\ , \tag{13}$$

$$A^{1ccl}_{000}=\frac{\max(l,c)}{[l]}\ , \tag{14}$$

$$\sum_c A^{Qccl}_{000}=1\ . \tag{15}$$

So any spectrum with a factor of about unity should be measurable, provided we can find an energy for which the appropriate radial integral(s) are large enough. For an interference term $c\neq c'$ the radial integrals R involved should be of about equal magnitude.

In the literature the derivation of the angular distribution is usually given in terms of linearly polarized light as a combination of $a=0$ and 2 polarizations. We can obtain this using

$$J^{\parallel}(\mathbf{P},\varepsilon)\equiv\tfrac{1}{3}[J^0(\mathbf{P},\varepsilon)-J^2(\mathbf{P},\varepsilon)]$$
$$=\tfrac{1}{3}\sum_{x\xi}I^x_\xi\sum_b[U^{0bx}_\xi B^{1l}_{0bx}-U^{2bx}_\xi B^{1l}_{2bx}]\ , \tag{16}$$

which directly gives the intensity for light linearly polarized ($q=0$) along **P**. Likewise the intensity for "unpolarized light" $[\frac{1}{2}(q=-1)+\frac{1}{2}(q=+1)]$ is

$$J^{\perp}(\mathbf{P},\varepsilon)\equiv\tfrac{1}{3}[J^0(\mathbf{P},\varepsilon)+\tfrac{1}{2}J^2(\mathbf{P},\varepsilon)]\ . \tag{17}$$

Alternatively, we may analyze the data using three spectra with mutually perpendicular polarization and so ob-

tain $J^0(\mathbf{P},\varepsilon)$ (which is independent of $\mathbf{P}$) and $J^2(\mathbf{P},\varepsilon)$ for $\mathbf{P}$ along the three directions. This procedure shows immediately that the sum of $J^2(\mathbf{P},\varepsilon)$ for $\mathbf{P}$ in three perpendicular directions is zero which is equivalent to the statement that the sum of the intensities for linear polarization in three arbitrary perpendicular directions gives the isotropic spectrum.

III. SPIN-POLARIZED THEORY

If we take the spin polarization of the emitted electron into consideration Eq. (1) becomes

$$|D_{qq'\sigma\sigma'}(\varepsilon)|^2=\sum_{mm'}\langle g|l^{\dagger}_{m\sigma}|f\rangle\langle f|l_{m'\sigma'}|g\rangle$$

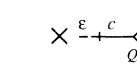

(18)

The spin of the emitted electrons is the same as that of the annihilated l electron. We have again, as in the case of q and q', introduced both σ and σ' in order to be able to consider spin measured in a direction other than the Z axis. In Eq. (1) the Z axis was sufficient because a sum over the two values of σ is independent of the direction. Recoupling gives

$$|D_{qq'\sigma\sigma'}(\varepsilon)|^2=\sum_{x\xi y\eta mm'\sigma\sigma'cc'}\langle g|l^{\dagger}_{m\sigma}|f\rangle\langle f|l_{m'\sigma'}|g\rangle(-1)^{l-m}\begin{pmatrix} l & x & l\\ -m & \xi & m'\end{pmatrix}(-1)^{1/2-\sigma}\begin{pmatrix}\frac{1}{2} & y & \frac{1}{2}\\ -\sigma & \eta & \sigma'\end{pmatrix}$$

$$\times\sum_{ab}[abx]\begin{Bmatrix} l & x & l\\ c & b & c'\\ Q & a & Q\end{Bmatrix}$$

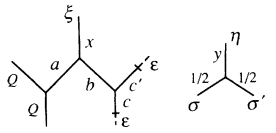

(19)

We see that we now measure the spectra

$$I^{xy}_{\xi\eta}\equiv n^{-1}_{lx}n^{-1}_{(1/2)y}\sum_{\sigma\sigma'mm'}\langle g|l^{\dagger}_{m\sigma}|f\rangle\langle f|l_{m'\sigma'}|g\rangle(-1)^{l-m}\begin{pmatrix} l & x & l\\ -m & \xi & m'\end{pmatrix}(-1)^{1/2-\sigma}\begin{pmatrix}\frac{1}{2} & y & \frac{1}{2}\\ -\sigma & \eta & \sigma'\end{pmatrix} \tag{20}$$

with the angle dependence

$$U^{Qabxy}_{qq'\xi\eta}(\varepsilon)=$$

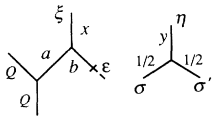

$$\underline{n}^{-1}_{abx}n^{-1}_{cbc'}\ . \tag{21}$$

To introduce explicitly the dependence on the light polarization vector $\mathbf{P}$ and the photoelectron spin direction $\mathbf{P}_S$ we again introduce linear combinations of the U factors, using as coefficients

$$r^{Qa}_{qq'}(\mathbf{P})r^{(1/2)y}_{\sigma\sigma'}(\mathbf{P}_S)\equiv n^{-1}_{Qa}$$

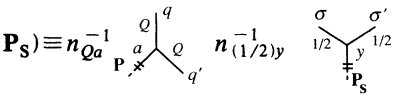

$$n^{-1}_{(1/2)y}$$

. (22)

The interpretation of these linear combinations for the photon part is the same as in Eq. (7), i.e., the photons are polarized along $\mathbf{P}$. For the spin part we take the coordinate Z axis along $\mathbf{P}_S$ and see from Table IV that for $y=0$ the signals for spin up and down along $\mathbf{P}_S$ are added, so this is the signal when we do not measure the spin polarization. For $y=1$ the signals are subtracted so the spin polarization along $\mathbf{P}_S$ is measured.

The angle dependence is then

$$U^{abxy}_{\xi\eta}(\mathbf{P},\varepsilon,\mathbf{P}_S)$$

$$=\underline{n}^{-1}_{abx}$$

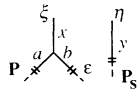

$$=\underline{n}^{-1}_{abx}\sum_{\alpha\beta}\begin{pmatrix} a & b & x\\ -\alpha & -\beta & \xi\end{pmatrix}C^a_{\alpha}(\mathbf{P})C^b_{\beta}(\varepsilon)C^y_{\eta}(\mathbf{P}_S)\ , \tag{23}$$

giving for the total intensity of photoelectrons in direction ε with spin detection along $\mathbf{P}_S$ using light with a polarization

$$J^{ay}(\mathbf{P},\varepsilon,\mathbf{P}_S)=\frac{1}{8\pi}\sum_{x\xi\eta}I^{xy}_{\xi\eta}C^y_{\eta}(\mathbf{P}_S)\sum_b U^{abx}_{\xi}(\mathbf{P},\varepsilon)B^{Ql}_{abx}\ . \tag{24}$$

Because the light acts on the orbit the waves emitted do not have the shape of the distribution of the annihilated electron ($b=x$) but also extra waves are emitted $b=|x-a|\cdots x+a$. For spin the emitted distribution (i.e., polarization direction) is the same as the distribution of the annihilated electron inside the atom, giving the simple shape of the spin part in Eq. (24).

In the case without spin-orbit coupling in the ground

TABLE IV. The values of $r^{(1/2)y}_{\sigma\sigma'}(\mathbf{Z})$ [Eq. (22)] which give the coefficients for spin up and spin down along $\mathbf{P}$ for measurement of the $y=0$ and 1 spectra.

$y\backslash\sigma$	-1	1
0	1	1
1	-1	1

and excited states the orbit and spin part are independent. This means that $I^{xy}_{\xi\eta}$ can be written as $I^{x}_{\xi} I^{y}_{\eta}$ with orbit and spin separated, or that if we measure the spectrum for spin-up minus spin-down along some quantization axis $\mathbf{P}_S$, the shape of the spectrum and the dependency on $\mathbf{P}_S$ is the same in any geometry $\mathbf{P},\varepsilon$. So the spin spectra can essentially be measured independent of the orbital part. The ratio of spin-polarized spectra and spin-unpolarized spectrum is independent of the kind of light and the emission direction.

When we do not observe such simple relations between the $I^{xy}_{\xi\eta}$ there must be spin-orbit coupling. Although all possible information is contained in the $I^{xy}_{\xi\eta}$, we again obtain more insight by taking suitable linear combinations

$$U^{abxy}_{\xi\eta}(\mathbf{P},\varepsilon,\mathbf{P}_S)=\sum_z [z]\underline{n}^{-1}_{abx}$$

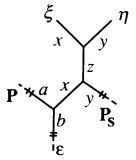

. (25)

We can incorporate one 3-j symbol and the summation over ξ and η into the spectrum

$$I^{xyz}_{\zeta}\equiv n^{-1}_{lx} n^{-1}_{(1/2)y} \underline{n}^{-1}_{xyz} \sum_{mm'\sigma\sigma'\xi\eta} \langle g|l^{\dagger}_{m\sigma}|f\rangle\langle f|l_{m'\sigma'}|g\rangle \begin{bmatrix} l & x & l \\ -m & \xi & m' \end{bmatrix} \begin{bmatrix} \frac{1}{2} & y & \frac{1}{2} \\ -\sigma & \eta & \sigma' \end{bmatrix} \begin{bmatrix} x & y & z \\ -\xi & -\eta & \zeta \end{bmatrix}, \quad (26)$$

with the angle dependence

$$U^{abxyz}_{\zeta}(\mathbf{P},\varepsilon,\mathbf{P}_S)=[z]\underline{n}^{-1}_{abx}\underline{n}^{-1}_{xyz}$$

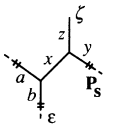

, (27)

$$J^{ay}(\mathbf{P},\varepsilon,\mathbf{P}_S)=\frac{1}{8\pi}\sum_{xz\zeta} n^2_{xyz} I^{xyz}_{\zeta} \sum_b U^{abxyz}_{\zeta}(\mathbf{P},\varepsilon,\mathbf{P}_S) B^{Ql}_{abx} . \quad (28)$$

The new spectra are linear combinations of the I^{xy}

$$I^{xyz}_{\zeta}=\sum_{\xi\eta} I^{xy}_{\xi\eta} \begin{bmatrix} x & y & z \\ \xi & \eta & \zeta \end{bmatrix} n^{-1}_{xyz} . \quad (29)$$

These combinations have as integrals ρ^{xyz}_{ζ} which give the coupling between the xth moment of the orbit with the yth moment of the spin. For $y=0$ we have the trivial case

$$\rho^{x0x}_{\zeta}=\rho^{x}_{\zeta} . \quad (30)$$

For $y=1$ we have, e.g.,

$$\rho^{011}_{\zeta}=S_{\zeta} , \quad (31)$$

$$\rho^{110}=\sum_i \langle l_i\cdot s_i\rangle , \quad (32)$$

which gives the spin-orbit coupling (mutual orientation of l and s),

$$\rho^{111}_{\zeta}=\sum_i \langle (l_i\times s_i)_{\zeta}\rangle , \quad (33)$$

which gives the "directed" angle between l and s,

$$\rho^{112}_{\zeta}=\sum_i \langle [l_i\times s_i]^2_{\zeta}\rangle , \quad (34)$$

which gives the mutual alignment (parallel versus perpendicular) of l and s.

These combinations allow one to study the spin of initial and final states, the spin-orbit coupling, etc., including the exotic ρ^{111}_{ζ}, which measures the average directed angle between l and s of the electrons. This will have a value when $\langle L\rangle$ and $\langle S\rangle$ have different directions, which could occur in a material that has L and S aligned to which we apply a magnetic field perpendicular to the easy direction. This might bend L and S in different angles because of their different mechanisms of anisotropy. The combinations with $x+y+z=$even with $x=0,1,2$ can also be studied in x-ray absorption[39] and angle-integrated photoemission.[3,4] In angle-resolved emission the range of x is extended and $x+y+z$ can be odd.

From Eqs. (32)–(34) we can see that the spin-orbit spectra can be obtained more directly from the experiment by analyzing the data in terms of coupled angular distributions. This should give us the possibility to find geometries that give a desired spectrum most sensitively. For example, for I^{110} the angle dependence is

$$U^{aby}(\mathbf{P},\varepsilon,\mathbf{P}_S)=$$

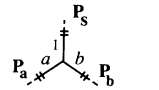

$$=\sum_{\alpha\beta\eta} C^{a}_{\alpha}(\mathbf{P}) C^{b}_{\beta}(\varepsilon) C^{y}_{\eta}(\mathbf{P}_S) \begin{bmatrix} a & b & y \\ -\alpha & -\beta & -\eta \end{bmatrix}, \quad (35)$$

with $y=1$. For aby we can have 101, 121, 221, so we can measure with circular polarization in even distributions for $\mathbf{P}$, ε, $\mathbf{P}_S$ or with linearly polarized light in the odd distribution $U^{221}(\mathbf{P},\varepsilon,\mathbf{P}_S)$, which means that $\mathbf{P}_S$ has to be outside the plane $\mathbf{P},\varepsilon$ (Sec. VII). In this way the spin-orbit spectrum $I^{110}=I^{11}_{1-1}+I^{11}_{00}+I^{11}_{-11}$ can be measured without measuring the $I^{11}_{\xi\eta}$ separately. The measurement of the other spectra is straightforward but because the waves now depend on four vectors (i.e., $\mathbf{P}$, ε, $\mathbf{P}_S$, and the $\mathbf{Z}$ axis) the strategy for finding optimal or even sufficient geometries to separate the spectra is highly technical and will not be considered here.

IV. CONTINUUM WITH NONSPHERICAL STRUCTURE

When the continuum levels are nonspherical because of interaction with the nonspherical environment of the atom (scattering) we obtain very generally

$$D_{qq'}(\varepsilon)=\sum_{mc\gamma k}\langle g|l^{\dagger}_{m\sigma}|f\rangle(-1)^{l-m}\begin{pmatrix} l & Q & c \\ -m & q & \gamma \end{pmatrix}\times R^{lQk}_{c\gamma}[lcc]^{1/2}n_{lQc}\ , \tag{36}$$

where k denotes the energy and angular quantum numbers of a continuum wave function which can be expanded into spherical harmonics at each distance r from the nucleus of the excited atom as

$$\Psi^{k}(\mathbf{r})=\sum_{c\gamma}\frac{1}{r}Y^{c}_{\gamma}(\mathbf{r}/r)P^{k}_{c\gamma}(r)\ , \tag{37}$$

producing a radial integral

$$R^{lQk}_{c\gamma}=\int dr\,P^{l}(r)r^{Q}P^{k}_{c\gamma}(r)\ , \tag{38}$$

where P^{l} is the radial part of the l-shell wave functions. The total intensity can be rewritten in the same way as Eq. (1) giving

$$J^{a}(\mathbf{P},\varepsilon)\propto\sum_{x\xi}I^{x}_{\xi}\sum_{bc\gamma c'\gamma'}\mathrm{P}^{\xi}_{x\,a\,b\,c\,c'\,\gamma\,\gamma'}A^{Qcc'l}_{abx}\sum_{kk'}R^{lQk}_{c\gamma}R^{lQk'}_{c'\gamma'}\Psi^{k}(\varepsilon)\Psi^{k'}(\varepsilon)\ . \tag{39}$$

Because the l level is again spherical, being a localized level, the intensity is still a linear combination of the same I^{x}_{ξ} but now with a more complicated angle dependence containing more parameters. The light is again an exact dipole and so a is still a relevant quantity.

We will not study here the degeneracy and symmetry of the $\Psi^{k}(\varepsilon)$ but only observe that in the presence of scattering very generally the study of localized level photoemission separates into two disciplines. The first discipline measures and studies the I^{x}_{ξ} which contain the physical information of the electronic structure of the atom independent of the kinetic energy. This discipline would preferably measure in a structureless continuum at constant kinetic energy. The other discipline measures and studies the continuum parameters which contain information on the potential of the ionized atom/molecule, which is directly connected to its geometry. This discipline would seem to be mostly interested in s core levels because even for an s shell which has interaction with the valence shell there is only one spectrum, i.e., I^{0}_{0} or in the case of spin polarization there are I^{00}_{00} and $I^{01}_{0\eta}$. This separation in disciplines is easily discernible in the literature and may serve to avoid confusion about the origin of new effects.

V. INTERPRETATION OF THE FUNDAMENTAL SPECTRA

Our formulas are given in terms of creation and annihilation operators in order to separate the analysis of angular distributions, which is merely a technical problem, from the analysis of the spectra, which is a problem for the quantum theoretician generally involving many-electron theory. For any theory it should be possible to calculate matrix elements of the annihilation operators. This has been done in paper II for LS coupled states in rare earths. The rest of the angular analysis is simply a one-electron calculation and so the theory of, e.g., Ref. 29 on the angular dependence of circular dichroism, which was demonstrated for one electron, is for a large part very general. By the use of the 2nd quantization formalism we are able to give a general analysis without considering details of individual cases. This is in contrast to the approach in paper I where we studied four different coupling schemes in order to find general properties.

We can consider

$$I_{mm'}\equiv\sum_{\sigma}\langle g|l^{\dagger}_{m\sigma}|f\rangle\langle f|l_{m'\sigma}|g\rangle\ , \tag{40}$$

as the fundamental properties of the system and determine them from Eq. (1). These $I_{mm'}$ contain the information about all one-electron properties connected with the shell l of the atom in the state $|g\rangle$ and also about the relationship between these properties of $|g\rangle$ and those of all the final states $|f\rangle$. The one-electron properties of the ground state are obtained by sum rules summing over all $|f\rangle$ using the closure relation. Although this formally represents an integral over the infinite energy range the only contributions to the sum will be from states $|f\rangle$ with one l electron less than $|g\rangle$, which are mainly in the part of the spectrum that we call l level photoemission. We thus obtain the elements of the one-electron density matrix

$$\rho_{mm'}\equiv\sum_{\sigma}\langle g|l^{\dagger}_{m\sigma}l_{m'\sigma}|g\rangle\ . \tag{41}$$

The $\rho_{mm'}$ contain all information about what electron states are occupied in $|g\rangle$ because they tell what states can be annihilated. This matrix is diagonal in cylindrical symmetry. In other symmetries diagonalization of this matrix gives the "natural orbitals" and the eigenvalues are their occupation numbers. The expectation value of any one-electron (orbital) operator T can be expressed in the $\rho_{mm'}$,

$$\langle T\rangle=\sum_{mm'}\rho_{mm'}\langle m|T|m'\rangle\ . \tag{42}$$

So we know everything about the shell l when we know all $\rho_{mm'}$. But in photoemission we do not directly measure the $\rho_{mm'}$ but rather the expectation values of certain operators which, by Eq. (42), are simple known linear combinations of them. Understanding these operators is important. First because they provide a direct physical intuition of what is measured and second, because by symmetry they normally contain such combinations of the $\rho_{mm'}$ that are nonzero while the rest are zero.

From Eq. (42) we see that the operators (or spectra)

that are naturally measured are the I^x_ξ. Measuring all the I^x_ξ allows us to calculate all $I_{mm'}$ if we would like to.

The integrals of the I^x_ξ are the ρ^x_ξ,

$$\rho^x_\xi \equiv n_{lx}^{-1} \sum_{mm'} \rho_{mm'} (-1)^{l-m} \begin{pmatrix} l & x & l \\ -m & \xi & m' \end{pmatrix} , \tag{43}$$

so

$$\rho^0_0 = \langle n_l \rangle , \tag{44}$$

$$\rho^1_\xi = \langle L_\xi \rangle l^{-1} , \tag{45}$$

$$\rho^2_\xi = \langle Q_\xi \rangle [\tfrac{1}{3} l(2l-1)]^{-1} . \tag{46}$$

These are the expectation values of the number of l electrons, the orbital angular momentum, and the quadrupole moment, respectively. The operators are normalized such that the $m=l$ diagonal matrix element of the zeroth component equals 1.

The I^x_ξ can be considered as the spectral decomposition of the operators ρ^x_ξ. The final states in the photoemission process are the "parents" of the ground state. That is, the ground state can be constructed by adding a suitable l electron to each final state and taking a linear combination of the resulting states. The I^x_ξ contain all the information on what l electron has been added to each final state. This is discussed in paper II. For example, the I^1_0 spectrum shows whether the added electron, which is the same as the escaping electron, has its orbital momentum parallel or antiparallel to other electrons. For final states with a high-L value the extra electron is antiparallel, and when it has a low-L value it is parallel. This shows why the I^x_ξ are the spectra we want.

In order to gain further understanding of the fundamental spectra and to give alternative ways to calculate them, we consider the expressions for the intensity for radiation with moments higher than dipole. When we consider l-pole radiation polarized along the Z axis, emitting l electrons into an s continuum level we obtain from Eq. (11) using Eqs. (A10) and (A13)

$$J^{la}(\mathbf{Z},\varepsilon) = \frac{1}{4\pi[l]} I^a_0 , \tag{47}$$

taking the radial integral to be 1. This is independent of ε (only $b=0$ is present). Therefore

$$I^x_0 = [l] \int d\varepsilon \, J^{lx}(\mathbf{Z},\varepsilon) , \tag{48}$$

which is the angle-integrated intensity for l-pole excitation to an s continuum and so from this formula we can calculate the I^a_0 without explicitly using creation and annihilation operators using l-pole radiation instead. This is trivial when $l=1$ and should be a simple extension in all those cases where one can already calculate dipole matrix elements. Only $\xi=0$ is found here because $b=0$ and $\mathbf{P}$ was along the Z axis. For other values of ξ we have to choose a different $\mathbf{P}$.

Until now we used creation and annihilation operators with azimuthal quantum numbers m and σ. For core levels with large spin-orbit coupling j and m_j are more interesting. For this we expand the operators

$$l_{m\sigma} \equiv a_{lm\sigma} = \sum_{jm_j} a_{ljm_j} [j]^{-1/2} (-1)^{j-m_j} \begin{pmatrix} l & \frac{1}{2} & j \\ m & \sigma & -m_j \end{pmatrix} , \tag{49}$$

and we obtain

$$I^x_\xi = \sum_{jm_j j'm'_j} n_{lx}^{-1} \langle g | a^\dagger_{ljm_j} | f \rangle \langle f | a_{lj'm'_j} | g \rangle$$

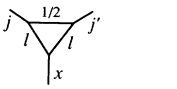

$$= \sum_{jm_j j'm'_j} n_{lx}^{-1} \langle g | a^\dagger_{ljm_j} | f \rangle \langle f | a_{lj'm'_j} | g \rangle$$

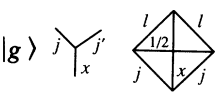

$$= \sum_{jm_j j'm'_j} n_{lx}^{-1} \langle g | a^\dagger_{ljm_j} | f \rangle \langle f | a_{lj'm'_j} | g \rangle (-1)^{j-m_j} \begin{pmatrix} j & x & j' \\ -m_j & \xi & m'_j \end{pmatrix} \begin{Bmatrix} j & x & j' \\ l & \frac{1}{2} & l \end{Bmatrix} . \tag{50}$$

In the limit of large spin-orbit coupling the $j=l-\frac{1}{2}$ edge is a region in the spectrum where the $|f\rangle$ have only holes with $j=j'=l-\frac{1}{2}$ and because of the triad (jxj) we have $0 \le x \le 2l-1$ which means that $x=2l$ is not present in the $j=l-\frac{1}{2}$ edge.

The fundamental spectra I^{xy} in papers I and II have been defined as special linear combinations of signals measured with polarized light and spin detection. Therefore these spectra differed (by a simple constant factor) for emission into $c=l+1$ and $c=l-1$. Our present definitions are made independent of c by dividing them by A_x. Further they are rescaled like in Eqs. (44)–(46) and so

$$I^{0y} = I^{0y}_o / A_0 , \tag{51}$$

$$I^{1y} = I^{1y}_o / (l A_1) , \tag{52}$$

$$I^{2y} = I^{2y}_o / [l(2l-1)/3 A_2] , \tag{53}$$

where the subscript o denotes the definitions in papers I and II. This means that the fundamental spectra for the $c=l-1$ channel are on the same relative scale as those in papers I and II, because

$$I^{xy}=(2l+1)I_0^{xy} \quad (c=l-1) . \tag{54}$$

Figures 2–5 show some results for the fundamental spectra of the rare earths in spherical symmetry calculated using the atomic multiplet program of Cowan.[40] It is clear that for every level each spectrum I^x has a unique structure describing the probabilities of reaching the final states of the atom by annihilation of electrons of a kind specified by x.

Figure 2 gives the example the $4f$ photoemission for the transition Yb $4f^{13}\rightarrow 4f^{12}\varepsilon d$. The Hund's rule ground state $4f^{13}\ ^2F_{7/2}$ ($M_J=-7/2$) is a single Slater determinant with $n_m=2$ for $-3\le m\le 2$ and $n_3=1$. Substitution of n_m into Eq. (43) and using Table III gives the integrated intensities $\rho^0=13$ and $\rho^{x\neq 0}=-1$.

Figure 3 shows the $4f$ photoemission for the transition Gd $4f^7\ ^8S_{7/2}$ ($M_J=-7/2$), where $n_m=1$ for all m, so that the integrated intensities of all fundamental spectra are zero, except I^0. However, the spin-orbit split J' level intensities still have a large x dependence.

Figure 4 shows the fundamental $3d$ core-level spectra for the transition Tm $4f^{12}\rightarrow 3d^9 4f^{12}\varepsilon p$. This spectrum is split by the large core-hole spin-orbit splitting into a $3d_{3/2}$ and $3d_{5/2}$ structure. The multiplet structure is due to the Coulomb and exchange interactions between the $3d$ and $4f$ electrons. The integrated intensities $\rho^{x\neq 0}$ are zero because the d shell is initially full. The I^4 spectrum is very small in the $3d_{3/2}$ edge because of the triad (jxj) in Eq. (50). The experimental core-level spectra may display large satellite structure due to hybridization in the initial and final state, however in this case our analysis in terms of fundamental spectra remains valid since it only assumes that the core shell is spherical.

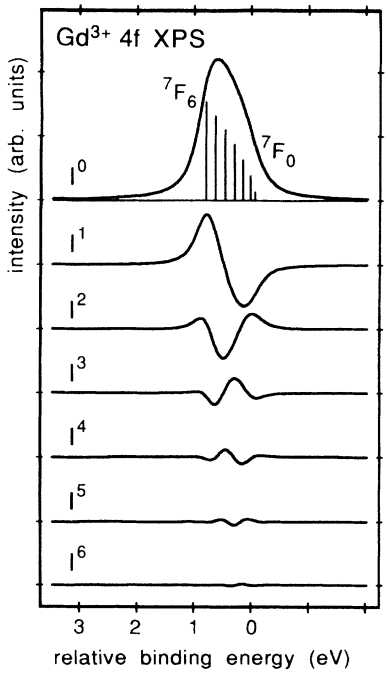

FIG. 3. The fundamental spectra for the photoemission Gd $4f^7\rightarrow 4f^6\varepsilon d$. Hartree-Fock parameters and convolution from paper II. All spectra are on the same scale.

Figure 5 shows the fundamental spectra calculated for the photoemission Tb $4f^8(^7F_6)\rightarrow 5p^5 4f^8\varepsilon s$. The isotropic spectrum shows a good agreement with the one measured by Thole *et al.*[41] The $5p$ spin-orbit splitting and the $4f$-$5p$ electrostatic interactions are of comparable or-

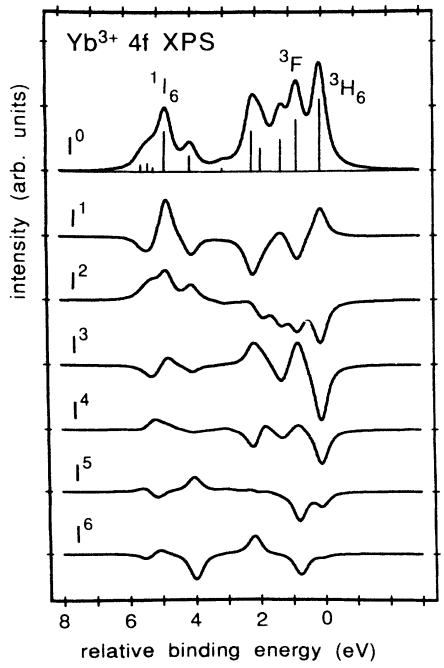

FIG. 2. The fundamental spectra for the photoemission Yb $4f^{13}\rightarrow 4f^{12}\varepsilon d$. Hartree-Fock parameters and convolution from paper II. All spectra are on the same scale.

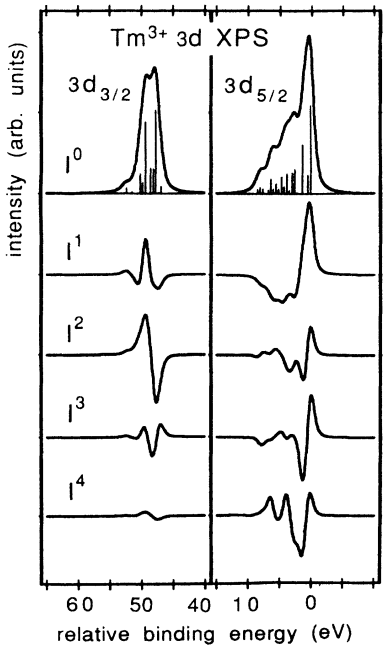

FIG. 4. The fundamental spectra for the photoemission Tm $4f^{12}\rightarrow 3d^9 4f^{12}\varepsilon p$. Hartree-Fock parameters from paper II and Ref. 55. Convolutions with a Lorentzian of $\Gamma=0.4$ and a Gaussian of $\sigma=0.4$ eV. All spectra are on the same scale.

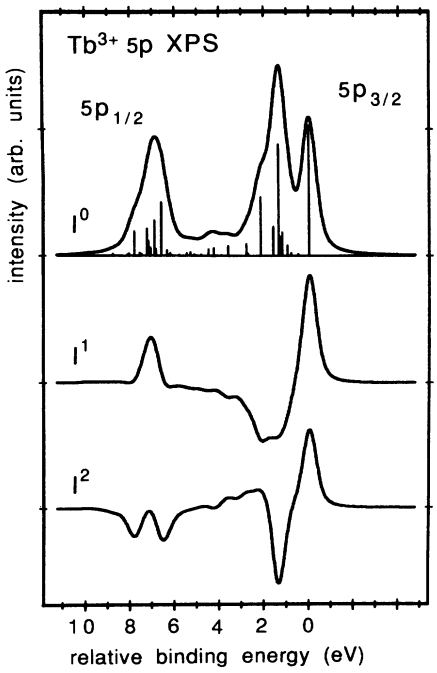

FIG. 5. The fundamental spectra for the photoemission Tb $4f^8(^7F_6)\rightarrow 5p^5 4f^8 \varepsilon s$. The Hartree-Fock values for the $4f^8$ configuration are $F^2=14.915$, $F^4=9.360$, $F^6=6.734$, $\zeta_f=0.221$ eV, and for the $5p^5 4f^8$ are $F^2(ff)=15.186$, $F^4(ff)=9.544$, $F^6(ff)=6.871$, $\zeta_f=0.224$, $\zeta_p=3.186$, $F^2(fp)=6.852$, $G^2(fp)=3.415$, and $G^4(fp)=2.673$ eV. Slater integrals were reduced to 80%. Convolution with a Lorentzian of $\Gamma=0.2$ a Gaussian of $\sigma=0.22$ eV. All spectra are on the same scale.

der of magnitude, so that the $5p_{1/2}$ and $5p_{3/2}$ characters are strongly mixed. For the p level there are only three fundamental spectra and in this case all spectra can be measured in angle-integrated photoemission.

VI. SYMMETRY OF THE ATOM

The theory in Sec. II is general in that it applies in any point-group symmetry. By assuming that we have only emission from the l shell, that we have dipolar radiation (which has moment 1) and that the continuum functions have no interaction with the lattice, we use the spherical symmetry to decide that there is only emission into $c=l\pm 1$, that we can use total moments a,b,x in the ranges $a=0\cdots 2$, $b=|c-c'|\cdots|c+c'|$, $x=0\cdots 2l$, and that a, b, and x have to fulfill the triangle relation. The parity symmetry $(-1)^l$ of functions of space limits b to even values and $a+b+x$ to even values for $c=c'$. This holds irrespective of whether the valence shell is localized or delocalized (we consider the l shell not to be a valence shell).

This use of O_3 as a supersymmetry only means that the orbitals and the light polarization we use are subspecies of (branch from) one single c, l, and Q value. A consequence is that there are $(2l+1)^2$ spectra for $x=0\cdots 2l$ and $\xi=-x\cdots x$, which means that the emission in $(2l+1)^2$ geometries has to be measured in order to separate them all.

Symmetry has the effect of making certain linear combinations of the I^x_ξ with the same x equal to zero and so we have to measure in correspondingly fewer geometries. We can see that only totally symmetric combinations contained in x are allowed by studying the symmetry properties of Eq. (3) where $|g\rangle$ and $|f\rangle$ belong to representations of the point group and the sum over the mm' is spherically symmetric (c.f. appendix). We can also understand it by considering the emission using isotropic light (e.g., three equally intense beams of X, Y, and Z polarization) so $a=0$ and $b=x$. Then the emitted intensity, which has a distribution with momentum x, must have the symmetry of the atom because the light can give no direction and so, when the atom is in equivalent positions we must obtain equal intensities. This means that x has to contain the totally symmetric representation of the point group. When the atom is spherical this means that only $x=0$ can contribute and thus only I^0_0 is nonzero. When the atom has cylindrical symmetry, e.g., a free atom in a magnetic field (along Z), then all x contribute but ξ has to be zero. So only the I^x_0 exist giving the $2l+1$ spectra called I^x in papers I and II which treated only cylindrical symmetry.

In other point groups there is a spectrum for every totally symmetric function contains in any x. We can see this and calculate the corresponding angle dependencies in the point group G when we expand the G symmetry functions $|l\Gamma\gamma\rangle$ into spherical harmonics $|lm\rangle$ (Ref. 42)

$$|l\Gamma\gamma\rangle=\sum_m |lm\rangle\langle lm|\Gamma\gamma\rangle\ , \tag{55}$$

where Γ is a representation of G and γ is a subspecies label needed when Γ is degenerate. Then if we consider as shorthand for Eq. (11) the intensity

$$J=\sum_{x\xi} I^x_\xi U^x_\xi=\sum_{x\Gamma\gamma\xi} I^x_\xi\langle x\xi|x\Gamma\gamma\rangle\langle x\Gamma\gamma|x\xi'\rangle U^x_{\xi'}\ , \tag{56}$$

we may define new linear combinations of the spectra and angle dependencies

$$I^x_{\Gamma\gamma}=\sum_\xi I^x_\xi\langle x\xi|x\Gamma\gamma\rangle\ , \tag{57}$$

$$U^x_{\Gamma\gamma}=\sum_\xi U^x_\xi\langle x\Gamma\gamma|x\xi\rangle\ , \tag{58}$$

and rewrite the intensity as

$$J=\sum_{x\Gamma\gamma} I^x_{\Gamma\gamma}U^x_{\Gamma\gamma}\ . \tag{59}$$

Because U has to be totally symmetric in G we must have $\Gamma\gamma=A_1$ and so

$$J=\sum_x I^x_{A_1}U^x_{A_1}\ . \tag{60}$$

When x branches to A_1 more than once we have

$$J=\sum_{xd} I^x_{A_1 d}U^x_{A_1 d}\ , \tag{61}$$

where d is a multiplicity label. This shows explicitly that the number of spectra is equal to the number of times $l\otimes l$ contains A_1. The spectra and their angle dependencies are given by Eqs. (57) and (58) with $\Gamma\gamma=A_1 d$.

Likewise, including again the photon polarization,

$$J^a(\varepsilon,\mathbf{P})=\frac{1}{4\pi}\sum_{xd} I^x_{A_1 d}\sum_b U^{abx}_{A_1 d}(\varepsilon,\mathbf{P})B^{Ql}_{abx}\ , \tag{62}$$

with

$$U^{abx}_{A_1 d}=\sum_\xi U^{abx}_\xi\langle x A_1 d|x\xi\rangle\ . \tag{63}$$

For the rare-earth compounds the splitting by the crystal field or magnetic field is so small that it cannot be resolved in the final state. In such a case, even though x (or z) may contain A_1 many times, the shape of the $I^x_{A_1 d}$ is independent of d and only its size changes proportionally to the expectation value of the corresponding operator. For example, in low symmetry X, Y, and Z are the A_1 component of $x=1$ and then the spectra I^1_X, I^1_Y, and I^1_Z have the same shape, but are proportional to $\langle L_X\rangle$, $\langle L_Y\rangle$, and $\langle L_Z\rangle$, respectively. Knowledge of this property reduces the number of data needed to measure the spectra. These can be calculated in any symmetry but SO_2 is the best choice because for each x it gives exactly one fundamental spectrum (c.f. Table V).

In the localized open shells of the $5f$ and $3d$ metal compounds the crystal-field interaction cannot be neglected and Table V gives the number of fundamental spectra. At high symmetry this is always small, e.g., the icosahedral symmetry gives only fundamental spectra for $x=0$ and 6. If we observe more spectra this must be due to lower symmetry, e.g., due to the surface. In O_h and T_d only $x=0$, 4, 6 contain A_1, so from a p core level there is only the isotropic spectrum and from a d level we have an additional spectrum from $x=4$, describing the difference between e and t_2 holes.

In the literature one often finds statements about the number of independent measurements necessary for a complete experiment. But those cases normally consider a completely known ground and excited state. Also in our case, if we have information on, e.g., the ground state such as its spin or symmetry we can use this to reduce the number of spectra and waves (angular distributions) to be taken into consideration.

VII. ANALYSIS OF ANGULAR DISTRIBUTIONS

From Eq. (11) we see the redundancy of the measurement. Consider measurement at one energy. Then for a chosen value of a each I^x_ξ sends out a set of different "waves" U^{abx}_ξ with $b=|x-a|\cdots x+a$ and b even. Thus for $a=0$ there is one wave, $b=x$, for each even x, for $a=1$ there is one, $b=x$, for each even x and there are about two, $b=x-1,x+1$ for each odd x. Likewise, for $a=2$ for each even x there are three values of b, $b=x-2,x,x+2$, and for each odd x there are two, viz., $b=x-1,x+1$. So for $a=0$ there is just enough information to obtain only the even x and $a=1$ is just sufficient to obtain the odd x but $a=1$ also contains twice the information for the even x and $a=2$ further increases the redundancy. If the R and δ were known then the relative intensities of the redundant waves would be fixed, so effectively each I^x_ξ sends out only one composite distribution. If the R and δ are considered unknowns then the relative coefficients would be determined by only two unknowns, the ratio between the two R values and the value of $\delta_c-\delta_{c'}$. The absolute value of the R cannot be determined because we may multiply the R with any (energy-dependent) factor and divide the I^x_ξ by its square and obtain the same intensity. If we treat the R and the δ as constant over the energy range we have only two parameters for the whole energy range. It would not be possible to solve for them by a measurement with $a=0$ alone because then there are as many waves as there are unknown I^x_ξ. (N.B. x is even only). But for $a=1$ and 2 there are more waves than unknowns. Because in solids we cannot do absolute intensity measurements, or only with great difficulty, we cannot determine the absolute values of the R nor determine the shape of the I^x_ξ to within an arbitrary function of energy. This is a serious drawback because much of the information we obtain from the spectra comes from the study of the shape and the satellite structure, which cannot be obtained from asymmetry parameters, as are usually determined in other disciplines. For example, for the application of sum rules for the I^x_ξ we need the shape of the spectrum. So in order to obtain the information we need we have to make assump-

TABLE V. Number of fundamental spectra in point-group symmetry. This is the number of times that x branches to the totally symmetric representation A_1 in the point group G.

$G\backslash x$	0	1	2	3	4	5	6	7
SO_3	1	0	0	0	0	0	0	0
K	1	0	0	0	0	0	1	0
O_h, T_d	1	0	0	0	1	0	1	0
D_6	1	0	1	0	1	0	2	0
D_4	1	0	1	0	2	1	2	1
D_3	1	0	1	1	2	1	3	2
D_2	1	0	2	1	3	2	4	3
SO_2	1	1	1	1	1	1	1	1
C_6	1	1	1	1	1	1	3	3
C_4	1	1	1	1	3	3	3	3
C_3	1	1	1	3	3	3	5	5
C_2	1	1	3	3	5	5	7	7
C_1	1	3	5	7	9	11	13	15

tions about the values of the R, e.g., that the largest one is constant or has a prescribed energy dependence. The ratio of the R will then be determined by fitting and may give a check on our assumptions. The variations in R are considerably smaller if we measure at constant photoelectron energy, scanning the photon energy, such as in constant final-state spectroscopy (CFS). This mode is probably preferable in any photoemission experiment but especially so in regions where R and δ vary strongly. The magnitude of these variations can be estimated from the tables of Goldberg, Fadley, and Kono.[43] Note that in many cases in the literature known initial and final states were considered to study R and δ measuring essentially U^{000} and U^{220} times the "simple" spectrum I^0. In our case we wish to consider R and δ as known and study the initial and final states.

For the analysis of angle dependence its symmetry properties will be important. From the symmetry section we know that the maximum number of different I^x_ξ is $(2l+1)^2$. By point-group symmetry this number is generally strongly reduced, e.g., to $2l+1$ in cylindrical symmetry where $\xi=0$. The angular distribution then contains correspondingly fewer waves and we need to measure in fewer geometries.

Parity is another important source of symmetry that simplifies the analysis. The intensity of U^{abx}_ξ changes sign whenever one of the vectors corresponding to an odd moment a, b, or x is inverted. For $\mathbf{P}$ and ε this can be seen from Eq. (8) because the spherical harmonics of odd moment have odd parity. At reversion of the magnetization $\mathbf{M}$ the U^{abx}_ξ do not change but all I^x_ξ with odd x (the magnetic spectra) change sign. Inverting an even moment does not change the signal. So because b is even inversion of ε never gives a change. When $a=1$ inversion of $\mathbf{P}$ is equivalent to exchanging left- and right-circularly polarized light and so the change of sign is trivial. The only interesting inversion is that of $\mathbf{M}$. We can separate odd and even values of x by reversing $\mathbf{M}$ and adding or subtracting the signals.

The above is valid in any symmetry but in any actual symmetry more can be said about equivalent geometries. In cylindrical symmetry we have $\xi=0$ and we may write

$$U^{abx}_\xi(\mathbf{P},\varepsilon)=\sum_\alpha \underline{n}^{-1}_{abx}\begin{vmatrix} a & b & x \\ -\alpha & \alpha & 0 \end{vmatrix} C^a_\alpha(\mathbf{P})C^b_{-\alpha}(\varepsilon)C^x_0(\mathbf{M})\ . \tag{64}$$

Because $\mathbf{M}$ is along the Z axis we have $C^x_\xi(\mathbf{M})=\delta_{\xi 0}$ and so

$$U^{abx}_\xi(\mathbf{P},\varepsilon)=\sum_{\alpha\beta\xi}\underline{n}^{-1}_{abx}\begin{vmatrix} a & b & x \\ -\alpha & -\beta & -\xi \end{vmatrix} C^a_\alpha(\mathbf{P})C^b_\beta(\varepsilon)C^x_\xi(\mathbf{M})$$
$$\equiv U^{abx}(\mathbf{P},\varepsilon,\mathbf{M})\ . \tag{65}$$

This function is totally symmetric for rotation of the coordinate system[44,45] and so $\mathbf{M}$ does not have to be along Z anymore; the result only depends on the angles between ε, $\mathbf{P}$, and $\mathbf{M}$. Using this property we can prove relatively easily that U is zero for certain geometries. The best known case is that of $a+b+x$ odd in a coplanar geometry. Here the intensity must be zero because when $a+b+x$ is odd one of the moments, say a, must be odd. Inverting that moment gives a change of sign. But the same geometry can be obtained by inverting b and x, which are even together and give no net sign change, and afterwards rotate 180° in the plane, which leaves U unchanged. Therefore $U=-U=0$. This result is usually expressed as the requirement that the geometry must be chiral to measure an odd wave. The same property is expressed by the fact[44] that an odd wave contains a factor $\varepsilon\cdot\mathbf{P}\times\mathbf{M}$ which is denoted s_{123} in Sec. VIII (Table IX). This factor is zero in a planar geometry. However it would suggest that the most chiral geometry is the one where ε, $\mathbf{P}$, and $\mathbf{M}$ are mutually perpendicular. This is not true when two of the moments, say b and x, are even. An even moment has no direction and may be denoted by two arrows in opposite directions. Then it is clear that the perpendicular geometry is equal to its mirror image and that it is not chiral. More generally: *The intensity of an odd wave with two even moments is zero when one of the even moments is perpendicular to the other two moments.* Formally this is proved by observing that inversion of the odd moment, which gives a sign change, followed by a rotation leads to the same geometry as inversion of the two even moments, which gives no sign change. The maximum intensity is obtained in a geometry in between coplanar and perpendicular.

The measurement of these odd waves, which occur only in interference $c=l\pm1$ gives two important applications which are not present in noninterference measurements. These are CDAD and what we will call MLDAD (magnetic linear dichroism in the angle dependence). In CDAD we use $a=1$ in order to measure even moments x. Odd moments, if the sample is magnetic, can be separated by reversing the magnetization. In MLDAD odd moments are studied using $a=0$ and 2. Even moments are again separated by reversing the magnetization.

We can show that *for even waves with two moments odd and one even the intensity is zero when one of the odd moments is perpendicular to the two other moments, which can make an arbitrary angle.* This is so because inversion of the two latter moments, which changes the sign because one of them is odd, leads to the same geometry as can be reached by a rotation.

When the point-group symmetry is not C_∞ the intensity does not only depend on the angles between $\mathbf{P}$, ε, and $\mathbf{M}$ but also on the angle of rotation of the atom around $\mathbf{M}$. When there is an axis of symmetry C_3 or higher all properties in C_∞ still hold for $x=1$. Then I^1_ξ is a vector which is oriented along the axis and has only a $\xi=0$ component when we take the symmetry axis as the Z-coordinate axis. When there is no symmetry, it is always possible to define the direction of $\mathbf{M}$ in the ground state, and we may normally assume that the final states will be quantized along the same direction. Then for $x=1$ the C_∞ analysis is still applicable. However for $x=2$ and higher it is not generally possible to choose a quantization axis which gives only $\xi=0$ components and then the atom has no rotational symmetry around the quantization axis and the full form U^{abx}_ξ has to be taken into consideration.

TABLE VI. The values of $A_{abx}^{Qcc'l}$ [Eq. (10)] for $l=1$.

	$cc'=00$	$cc'=20$			$cc'=22$			
$(ab0)$ $A_{ab0}^{lc'1}$	(000) $\frac{1}{3}$	(220) $\frac{-2}{3}$			(000) $\frac{2}{3}$	(220) $\frac{-2}{3}$		
$(ab1)$ $A_{ab1}^{1cc'1}$	(101) $\frac{1}{3}$	(121) $\frac{-1}{3}$	(221) $\frac{5}{4}i$		(101) $\frac{-1}{3}$	(121) $\frac{2}{3}$		
$(ab2)$ $A_{ab2}^{1cc'1}$	(202) $\frac{1}{3}$	(022) $\frac{-1}{3}$	(122) $\frac{5}{12}i$	(222) $\frac{1}{3}$	(022) $\frac{-1}{3}$	(202) $\frac{1}{15}$	(222) $\frac{-2}{21}$	(242) $\frac{36}{35}$

VIII. APPLICATIONS

The angular dependence of J^a is given by Eq. (11) where only a finite number of waves U_{ξ}^{abx} can contribute because a, b, x, and ξ are restricted by momentum coupling and symmetry. For p, d, and f photoemission the allowed values of $A_{abx}^{1cc'l}$ [Eq. (10)] are given in Tables VI, VII, and VIII, respectively, where they are ordered in rows of increasing x, corresponding with the fundamental spectra I_{ξ}^{x}. The imaginary values of A can only be measured in chiral geometry. The three columns cc' in the tables correspond to the $l-1$ channel, the interference term, and the $l+1$ channel. Values for the R and δ can be found in, e.g., Ref. 43.

It is instructive to show the relation between the $A_{abx}^{1cc'l}$ values and the values A_x derived in Paper II (Table I) for angle-integrated photoemission. Due to the factor in Eq. (9) and a different normalization [see Eqs. (51)–(54)] of the operators in Eqs. (44)–(46) A_x is not equal to A_{x0x}^{1cci} but

$$A_{000}^{1ccl}=l_{>}A_0 , \tag{66}$$

$$A_{101}^{1ccl}=l_{>}lA_1 , \tag{67}$$

$$A_{202}^{1ccl}=l_{>}l(2l-1)/3A_2 , \tag{68}$$

where

$$l_{>}=[lc]n_{l1c}^{2}=\max(l,c) . \tag{69}$$

A. Angle dependence in p photoemission

As an example we will now write out the angle dependence of emission from a p level for dipole radiation and discuss three cases from the literature. We will only consider cylindrical symmetry and so ξ is zero.

$$\begin{aligned}4\pi J^0&=I^0U^{000}(A_{000}^{1001}R^{00}+A_{000}^{1221}R^{22})+I^2U^{022}[A_{022}^{1201}(R^{20}+R^{02})+A_{022}^{1221}R^{22}]\\&=I^0(\tfrac{1}{3}R^{00}+\tfrac{2}{3}R^{22})+I^2(\tfrac{3}{2}c_1^2-\tfrac{1}{2})[-\tfrac{2}{3}(R^0R^2\cos\delta)-\tfrac{1}{3}R^{22}] ,\end{aligned} \tag{70}$$

$$\begin{aligned}4\pi J^1&=I^1[U^{101}(\tfrac{1}{3}R^{00}-\tfrac{1}{3}R^{22})+U^{121}(-\tfrac{2}{3}R^0R^2\cos\delta+\tfrac{2}{3}R^{22})]+I^2U^{122}(\tfrac{5}{6}R^0R^2\sin\delta)\\&=I^1[c_2(\tfrac{1}{3}R^{00}-\tfrac{1}{3}R^{22})+(\tfrac{3}{2}c_1c_3-\tfrac{1}{2}c_2)(-\tfrac{2}{3}R^0R^2\cos\delta+\tfrac{2}{3}R^{22})]+I^2c_1s_{123}R^0R^2\sin\delta ,\end{aligned} \tag{71}$$

$$\begin{aligned}4\pi J^2&=I^0U^{220}[-\tfrac{2}{3}(R^{02}+R^{20})-\tfrac{2}{3}R^{22}]+I^1U^{221}[\tfrac{5}{4}i(R^{02}-R^{20})]\\&\quad+I^2[U^{202}(\tfrac{1}{3}R^{00}+\tfrac{1}{15}R^{22})+U^{222}(\tfrac{2}{3}R^0R^2\cos\delta-\tfrac{2}{21}R^{22})+U^{242}(\tfrac{36}{35}R^{22})]\\&=I^0(\tfrac{3}{2}c_3^2-\tfrac{1}{2})(-\tfrac{4}{3}R^0R^2\cos\delta-\tfrac{2}{3}R^{22})+I^1(-\tfrac{3}{2}s_{123}c_3)(R^0R^2\sin\delta)+I^2(\cdots) ,\end{aligned} \tag{72}$$

where $\delta\equiv\delta_0-\delta_2$, $R^{cc'}\equiv R^cR^{c'}e^{i(\delta_c-\delta_{c'})}$, and s_{123} and angles c_1,c_2,c_3 are defined in Table IX. U^{abx} is used here for $U_0^{abx}(\mathbf{P},\varepsilon,\mathbf{Z})$ taking the magnetization to be along $\mathbf{Z}$.

Because for in-plane geometries U^{122} is zero J^1 is then purely proportional to I^1. Neglecting the spectrum I^2 (which is small in the $j=\frac{1}{2}$ edge, c.f. Sec. V) and the transition to the s continuum ($R^0=0$) we can compare to Ref. 29,

$$4\pi J^0=I^0(\tfrac{2}{3})R^{22} , \tag{73}$$

$$4\pi J^1=I^1(\tfrac{2}{3}c_2-c_1c_3)R^{22} , \tag{74}$$

$$4\pi J^2=I^0(\tfrac{1}{3}-c_2^2)R^{22} , \tag{75}$$

$$\frac{J^1}{J^{\perp}}=\frac{I^1}{I^0}\frac{(\frac{2}{3}c_2-c_1c_3)}{\frac{1}{3}(\frac{5}{6}-\frac{1}{2}c_1^2)} . \tag{76}$$

This is the same angle dependence as given in Ref. 29 and 46.

Schneider and co-workers[29,30] have measured the angular dependence of the circular dichroism of the $2p$ core level of ferromagnetic iron. The prediction by the theory that for coplanar geometries there is only one spectrum, i.e., I_0^1, seems to be confirmed. However, the authors plot and analyze the asymmetry ratio $\frac{1}{2}J^1/J^{\perp}$, which is not well suited for our analysis in terms of linear combinations of fundamental spectra. For the angle dependence of the magnitude of the signal the authors use a one-

TABLE VII. The values of $A_{abx}^{Qcc'l}$ [Eq. (10)] for $l=2$.

	$cc'=11$			$cc'=13$				$cc'=33$			
$(ab0)$	(000)	(220)		(220)				(000)	(220)		
$A_{ab0}^{1cc'2}$	$\frac{2}{5}$	$\frac{-2}{25}$		$\frac{-18}{25}$				$\frac{3}{5}$	$\frac{-12}{25}$		
$(ab1)$	(101)	(121)		(121)	(221)			(101)	(121)		
$A_{ab1}^{1cc'2}$	$\frac{2}{5}$	$\frac{-4}{25}$		$\frac{-6}{25}$	$\frac{3}{2}i$			$\frac{-2}{5}$	$\frac{16}{25}$		
$(ab2)$	(022)	(202)	(222)	(022)	(122)	(222)	(242)	(022)	(202)	(222)	(242)
$A_{ab2}^{1cc'2}$	$\frac{-2}{5}$	$\frac{2}{5}$	$\frac{-4}{35}$	$\frac{-6}{35}$	$\frac{5}{14}i$	$\frac{138}{245}$	$\frac{72}{245}$	$\frac{-24}{35}$	$\frac{6}{35}$	$\frac{-48}{245}$	$\frac{216}{245}$
$(ab3)$	(123)			(123)	(143)	(223)	(243)	(123)	(143)		
$a_{ab3}^{1cc'2}$	$\frac{-6}{25}$			$\frac{12}{175}$	$\frac{6}{35}$	$\frac{-1}{4}i$	$\frac{-9}{20}i$	$\frac{18}{175}$	$\frac{-12}{35}$		
$(ab4)$	(224)			(044)	(144)	(224)	(244)	(044)	(224)	(244)	(264)
$A_{ab4}^{1cc'2}$	$\frac{-36}{175}$			$\frac{6}{35}$	$\frac{-27}{140}i$	$\frac{-18}{1225}$	$\frac{-6}{49}$	$\frac{3}{35}$	$\frac{-12}{1225}$	$\frac{12}{539}$	$\frac{-30}{77}$

electron-like model which fixes the ratio of the I^0, I^1, and I^2 spectra by assuming the $m_j=\pm\frac{3}{2}$ levels to be degenerate with $m_j=\pm\frac{1}{2}$. In a many-particle model these ratios may be different and vary with the final state, influencing the J^1 angle dependence which appears in the asymmetry. So it is hard to judge whether the deviations from their model fit into our theory.

Another case is the $5p$ emission of rare earths between 0 and 100 eV above threshold.[47,48] Assuming only I^0 to be nonzero we have

$$4\pi J^{\parallel}=\tfrac{1}{9}I^0[R^{00}+(6c_3^2-2)R^0R^2\cos\delta+(3c_3^2+1)R^{22}]\ . \tag{77}$$

When the R and δ are constants we measure an undistorted I^0, but when they vary with energy the I^0 appears distorted because it is multiplied by an energy-dependent function. But when R^0 and R^2 are different functions of energy the distortion depends on c_3 which is the cosine of the angle between light polarization and emission direction. This is indeed the case in the energy region considered and a change in peak ratio can be produced by this effect. In order to analyze these spectra this effect should be taken into account, e.g., by making an assumption about one of the parameters R^0, R^2, and $\cos\delta$ and measuring at a few different values of c_3. It may be simpler to measure in constant final-state (CFS) mode, where the parameters are expected to be much more constant.

B. MLDAD in p photoemission

In a recent experiment by Roth *et al.*[26] a different emission intensity was measured with linearly polarized

TABLE VIII. The values of $A_{abx}^{Qcc'l}$ [Eq. (10)] for $l=3$.

	$cc'=22$				$cc'=24$					$cc'=44$			
$(ab0)$	(000)	(220)			(220)					(000)	(220)		
$A_{ab0}^{1cc'3}$	$\frac{3}{7}$	$\frac{-6}{49}$			$\frac{-36}{49}$					$\frac{4}{7}$	$\frac{-20}{49}$		
$(ab1)$	(101)	(121)			(121)	(221)				(101)	(121)		
$A_{ab1}^{1cc'3}$	$\frac{3}{7}$	$\frac{-12}{49}$			$\frac{-9}{49}$	$\frac{45}{28}i$				$\frac{-3}{7}$	$\frac{30}{49}$		
$(ab2)$	(022)	(202)	(222)	(242)	(022)	(122)	(222)	(242)		(022)	(202)	(222)	(242)
$A_{ab2}^{1cc'3}$	$\frac{-30}{49}$	$\frac{3}{7}$	$\frac{-60}{343}$	$\frac{18}{343}$	$\frac{-5}{49}$	$\frac{25}{84}i$	$\frac{235}{343}$	$\frac{150}{343}$		$\frac{-125}{147}$	$\frac{5}{21}$	$\frac{-250}{1029}$	$\frac{270}{343}$
$(ab3)$	(123)	(143)			(123)	(143)	(223)	(243)		(123)	(143)		
$A_{ab3}^{1cc'3}$	$\frac{-18}{49}$	$\frac{4}{49}$			$\frac{4}{49}$	$\frac{10}{49}$	$\frac{-5}{12}i$	$\frac{-3}{4}i$		$\frac{10}{49}$	$\frac{-24}{49}$		
$(ab4)$	(044)	(224)	(244)		(044)	(144)	(224)	(244)	(264)	(044)	(224)	(244)	(264)
$A_{ab4}^{1cc'3}$	$\frac{9}{49}$	$\frac{-108}{343}$	$\frac{180}{3773}$		$\frac{90}{539}$	$\frac{-81}{308}i$	$\frac{-18}{343}$	$\frac{-11430}{41503}$	$\frac{-90}{847}$	$\frac{162}{539}$	$\frac{-180}{3773}$	$\frac{3240}{41503}$	$\frac{-450}{847}$
$(ab5)$	(145)				(145)	(165)	(245)	(265)		(145)	(165)		
$A_{ab5}^{1cc'3}$	$\frac{5}{49}$				$\frac{-20}{539}$	$\frac{-5}{77}$	$\frac{3}{28}i$	$\frac{13}{84}i$		$\frac{-15}{539}$	$\frac{10}{77}$		
$(ab6)$	(246)				(066)	(166)	(246)	(266)		(066)	(246)	(266)	(286)
$A_{ab6}^{1cc'3}$	$\frac{45}{539}$				$\frac{-5}{77}$	$\frac{65}{924}i$	$\frac{30}{5929}$	$\frac{5}{121}$		$\frac{-5}{231}$	$\frac{135}{77077}$	$\frac{-2}{363}$	$\frac{56}{429}$

TABLE IX. The function $U^{l_1 l_2 l_3}(\mathbf{P}_1,\mathbf{P}_2,\mathbf{P}_3)$ where $c_1=\mathbf{P}_2\cdot\mathbf{P}_3$, $c_2=\mathbf{P}_3\cdot\mathbf{P}_1$, $c_3=\mathbf{P}_1\cdot\mathbf{P}_2$ and $s_{123}=\mathbf{P}_1\cdot(\mathbf{P}_2\times\mathbf{P}_3)$, which is the volume of a block spanned by $\mathbf{P}_1$, $\mathbf{P}_2$, and $\mathbf{P}_3$. Other functions can be obtained by permutation of 1, 2, and 3. Note that an odd permutation changes the sign of $s_{123}=-s_{213}=\cdots$. The forms given here are nicely symmetric in 1, 2, and 3 but especially the forms with high l values are difficult to analyze and plot. For those purposes the original expressions Eq. (70)–(72) evaluated by computer with $\mathbf{P}_1$ along $\mathbf{Z}$ and $\mathbf{P}_2$ in the XY plane are more suited, although they are unsymmetric.

$U^{000}=1$
$U^{011}=c_1$
$U^{022}=\frac{3}{2}c_1^2-\frac{1}{2}$
$U^{112}=\frac{3}{2}c_1c_2-\frac{1}{3}c_3$
$U^{222}=\frac{1}{2}(2-3c_1^2-3c_2^2-3c_3^2+9c_1c_2c_3)$
$U^{242}=\frac{1}{8}(1-5c_1^2+2c_2^2-5c_3^2-20c_1c_2c_3+35c_1^2c_3^2)$
$U^{122}=\frac{6}{5}c_1s_{123}$

light ($a=0$ and 2, so a is even) when the magnetization was reversed which means that there must be a term with an odd value for x. From Eq. (72) we see that this has to be the term with I^1U^{221}. This term, like any term with a even and x odd, has an odd angular dependence and so there is no signal when light polarization, magnetization and emission direction are coplanar. Indeed in the geometry used the light polarization was 16° out of the ε, **M** plane. We expect for the intensity difference

$$\Delta J^{\parallel}=\frac{1}{3}(\Delta J^0-\Delta J^2)$$

$$=\frac{1}{3}\Delta J^2=\frac{2}{3}\frac{1}{4\pi}I^1\frac{3}{2}c_3s_{123}R^0R^2\sin\delta\ . \qquad (78)$$

The angle dependence is c_3s_{123}, which has its maximum value of 0.5 when $\theta\equiv\angle(\varepsilon,\mathbf{P})=45°$ and **M** is perpendicular to the plane ε,**P**. When $\theta=16°$ the value of $c_3s_{123}=0.265$. Therefore we expect that the effect can be increased further. The important conclusion here is that with linear dichroism in the interference channel we in fact measure the I^1 spectrum, the same spectrum one measures with circularly polarized light in coplanar geometry (by U^{101} and U^{121}). It is the counterpart of the term U^{122} which measures I^2 using circularly polarized light in an off-plane geometry (CDAD).

C. Angle dependence in *f* photoemission

Recently Starke *et al.*[49] measured the circular dichroism in Gd 4*f* photoemission. We will now give the angle dependence assuming that only the $f\rightarrow g$ channel contributes and that I^5 does not contribute because its coefficients are too small (see Table VIII).

$$4\pi J^1=[I^1(-\tfrac{3}{7}U^{101}+\tfrac{30}{49}U^{121})+I^3(\tfrac{10}{49}U^{123}-\tfrac{24}{49}U^{143})]R^{44}\ , \qquad (79)$$

We have plotted the coefficient of I^1 and I^3 in Fig. 6, which shows that Starke *et al.* indeed measured almost purely I^1 and that configuration ○ is best suited to measure I^3.

From Table VIII, we see that also measurement in LDAD looks promising in the region that the *d* channel contributes, especially the coefficients for U^{221} and U^{243}. A drawback is that the *d* channel only contributes up to about 10 eV above the edge[43] where interaction of the continuum level with the lattice may complicate the analysis.

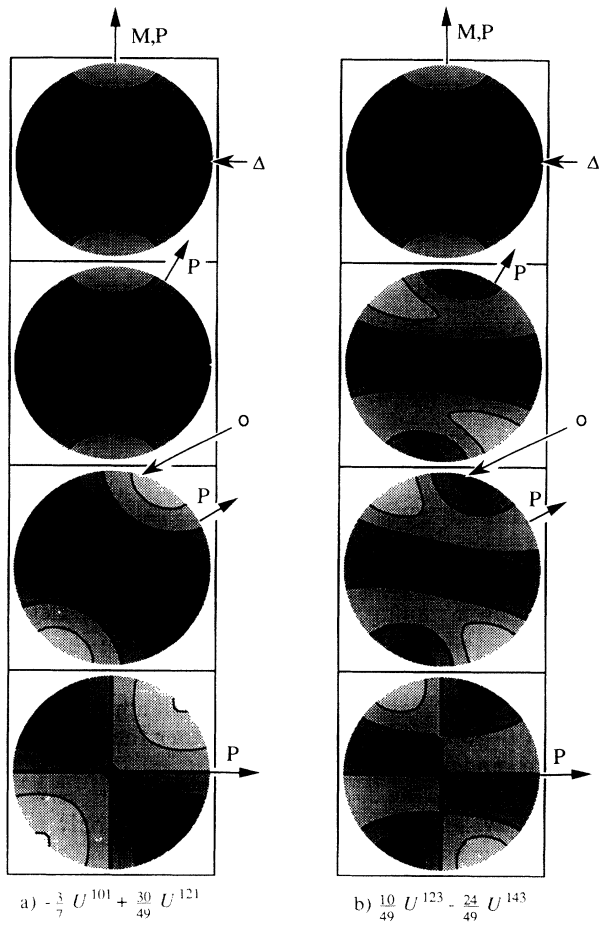

FIG. 6. Angular distribution of the coefficients for (a) I^1 and (b) I^3 in Eq. (79). The plots show the emission intensity from a viewpoint perpendicular to the **P**,**M** plane. In the four plots **M** is always in the vertical direction pointing upward while **P** is at 0, 30, 60, and 90° with **M**. The center of the circle gives the intensity in the direction perpendicular to the **P**, **M** plane. The radius of a plotted point is its polar angle with this direction. Thus the boundary of the circle gives the emission in **P**,**M** plane. The contours have intervals of 0.2, where the thick lines are the contours of zero intensity. Dark (light) grey denotes negative (positive) intensity. The approximate geometry used by Starke *et al.* (Ref. 49) is indicated by △. A geometry suitable for measuring I^3 is indicated by ○.

IX. CONCLUSIONS

Recent experimental work by Schneider, Venus, and Kirschner[29] and Roth *et al.*[26] have kindled the interest in magnetic circular and linear dichroism in the angle-resolved core-level photoemission from magnetic ordered materials. We have presented a general model, where we derived the angular dependence of photoemission from

localized shells in the limit of spherical continuum states.

The angular anisotropy of the emission from a core level is due to the polarization of the photon and to the electrostatic interaction between the hole created and the polarized valence electrons. In emission from a localized open shell an additional anisotropy is caused by the initial polarization of the shell from which the electron is emitted. In x-ray absorption and angle-integrated photoemission we can obtain the occupation number, the magnetic orientation $\langle M \rangle$ and the magnetic alignment $\langle M^2 \rangle$ by measuring the isotropic, the circular dichroism, and linear dichroism, respectively. However, in angle-dependent photoemission, where the photoelectron distribution carries away a higher momentum, we can observe all moments up to $\langle M^{2l} \rangle$ or, with spin-orbit coupling, up to $\langle M^{2l,1} \rangle$.

The expression for the angular-dependent photoemission can be written as a sum over energy-dependent factors, which are the fundamental spectra containing all the physical information about the many-electron system. In each geometry we measure a linear combination of the same set of fundamental spectra. For example, in cylinder symmetry the emission from a localized shell l measured at an arbitrary emission angle is always a linear combination of $2l+1$ fundamental spectra. Each fundamental spectrum produces a limited set of angular waves. These waves are a function of the angles between the photon polarization, the magnetic orientation and the emission direction. Special effects can occur when the geometry spanned by these vectors is chiral and there is appreciable signal in the interference between the $l-1$ and $l+1$ channels. Whereas in a nonchiral geometry we measure even moments with isotropic or linearly polarized light, and odd (i.e., magnetic) moments with circularly polarized light, in a chiral geometry we measure even moments with circularly polarized light and odd moments with linearly polarized light. The moment analysis reveals the relation between these apparently uncorrelated experiments. For example, the spectrum I^{10} which is the magnetic dichroism usually measured with circular polarization can also be measured by MLDAD which uses linear polarization in a nonplanar geometry. The latter measurement is more advantageous because linearly polarized synchrotron radiation has much more intensity and higher degree of polarization than its circularly polarized companion. Moreover, MLDAD can even be measured with "unpolarized" radiation.

We have shown how the angular dependence of these spectra can be calculated in a simple and straightforward way. This can be helpful to find those emission angles which give the most intense fundamental spectra, i.e., the strongest polarization effects and to find the *magic angles* for which certain fundamental spectra are zero. The magnitude of the different fundamental spectra and their coefficients do not vary strongly so that each of them can be measured in some geometry except for the I^5 and I^6 spectra of f shells which have very small coefficients.

Scattering by the environment can be included, but will introduce additional parameters which make the analysis less transparent. The influence of the potential has been evidenced in CO adsorbate on a metal surface by the presence of a CDAD effect in the C $1s$ photoemission due to the interference between the transitions to the $p\pi$ and $p\sigma$ continua.[50] We have only given a complete description of the first step, the excitation process from a localized shell. Further developments of the theory of scattering mechanisms are highly desirable, and could push the advancement of photoelectron diffraction and photoelectron holography of magnetic materials.

In our analysis we have shown how to separate the geometric factor from the spectra which give the physical properties of the atom. The angular distribution can be derived in a one-electron calculation since the photon and the angle distribution act on the same electron. The analysis is valid both for one-electron and for many-electron systems. In paper I we used different derivations for the various coupling cases in order to understand the fundamental spectra. Here we use a second quantization formalism which has the great advantage that the analysis is valid independent of the theory that may be necessary to describe the valence shell and its interactions with the localized shell: Whether the theoretical analysis has to be done in band-structure theory or by a localized approach in any coupling scheme has no influence on the way the experimental data have to be treated.

Spin-polarization measurements can be treated in the same formalism and gives information on the spin and its correlations with the orbital moments, such as spin-orbit coupling. The technique of the analysis is the same but it is more tedious.

APPENDIX

We give our fundamental spectra as being a function of the final state $|f\rangle$. We can obtain the intensity as a function of photon energy ω, photoelectron energy E, and initial and final-state energies E_g and E_f using

$$I(E,\omega) \equiv \sum_f I(f)\delta(E+E_f-\omega-E_g) . \tag{A1}$$

The measured intensity also contains radial integrals which are a function of E. Our fundamental spectra do not contain these and are a function of $E-\omega$. In order to obtain the integral over the fundamental spectrum we can use

$$\int I(E,\omega)dE = \int I(E,\omega)d\omega = \sum_f I(f) . \tag{A2}$$

Further, when g and f are degenerate we implicitly assume a sum over the degenerate levels or over the Boltzmann distribution of g. This makes our spectra totally symmetric where needed. Finally summation of the spectra for equivalent sites produces a total spectrum which has the symmetry of the crystal (or lower when the surface contribution is important).

The structure of angle dependencies is more clearly shown if we use a graphical representation for the (normalized) spherical harmonics. We use

$$Y_m^l(\varepsilon) = {}_m\overset{l}{\longrightarrow}\overset{\varepsilon}{+} , \tag{A3}$$

where ε is a unit vector, or it may be considered to

represent, e.g., polar angles (ϑ,φ). For normalized spherical harmonics we use a double cross bar

$$C_m^l(\varepsilon)\equiv\left[\frac{4\pi}{2l+1}\right]^{1/2}Y_m^l(\varepsilon)= \quad . \tag{A4}$$

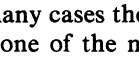

Equation (8) shows an example of how to combine 3-j symbols and spherical harmonics. A standard operation is the coupling of two spherical harmonics of the same vector, e.g., in Eq. (4)

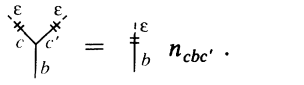

$$= n_{cbc'} \, . \tag{A5}$$

This can also be used to simplify the angle dependence in Eq. (8) for special cases. For example, when $\mathbf{P}\|\varepsilon$:

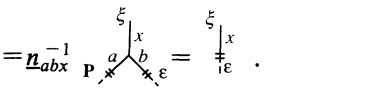

$$U^{abx}_{\xi}(\mathbf{P}\|\varepsilon)=\underline{n}^{-1}_{abx} \quad . \tag{A6}$$

This is essentially the result of Goldberg, Fadley, and Kono[51]. Here we have expanded their square of a spherical harmonic into spherical harmonics.

For the normalization of the fundamental spectra we define a numerical factor (c.f. Ref. 52)

$$n_{lx}\equiv\begin{bmatrix} l & x & l \\ -l & 0 & l \end{bmatrix}=\frac{(2l)!}{\sqrt{(2l-x)!(2l+1+x)!}} \, , \tag{A7}$$

For the normalization of the angle dependence we define the factors

$$n_{abc}\equiv\begin{bmatrix} a & b & c \\ 0 & 0 & 0 \end{bmatrix} \, , \tag{A8}$$

$$\underline{n}_{abx}=i^g\left[\frac{(g-2a)!(g-2b)!(g-2x)!}{(g+1)!}\right]^{1/2} \times\frac{g!!}{(g-2a)!!(g-2b)!!(g-2x)!!} \, , \tag{A9}$$

where $g=a+b+x$. When g is even we have $\underline{n}_{abx}=n_{abx}$, but when g is odd $n_{abx}=0$. So Eq. (A9) is a natural "extrapolation" of n_{abx}. Because of the factor i^g, $\underline{n}$ is imaginary when g is odd. This nicely cancels the factor i present in the rest of the angle dependence. It appears again in the A factor where it combines with the complex phase shift factor to make it real. When one of the moments is zero we have the special values

$$n_{l0}=\underline{n}_{ll0}=(2l+1)^{-1/2} \, . \tag{A10}$$

We have introduced such normalizations that make all quantities rational numbers, removing all square roots. This can always be achieved by balancing every triad $(l_1l_2l_3)$ in all $3n$-j symbols by a corresponding $\Delta(l_1l_2l_3)$

$$\Delta(l_1l_2l_3)=\left[\frac{(L-2l_1)!(L-2l_2)!(L-2l_3)!}{(L+1)!}\right]^{1/2} \, , \tag{A11}$$

where $L=l_1+l_2+l_3$. So, e.g., a 9-j symbol can be multiplied or divided by six Δ factors to make the result rational.[53] Instead of a Δ factor 3-j symbols of the forms

$$\begin{bmatrix} l & x & l \\ -m & 0 & m \end{bmatrix} \quad \text{or} \quad \begin{bmatrix} a & b & x \\ 0 & 0 & 0 \end{bmatrix} \, , \tag{A12}$$

such as our n_{lx} and $n_{cbc'}$ factors, can be used which are a rational factor times a Δ factor. These factors often appear as natural normalization factors as, e.g., the n_{Qa} factor in Eq. (7), but in complicated problems the search for the correct Δ factor can give a clue to the solution.

In many cases there are "degenerate" triads $(a,b,a+b)$ where one of the moments is the sum of the other two. Then we can often obtain simple formulas,[54] e.g.,

$$\begin{Bmatrix} l & x & l \\ c & b & c \\ Q & a & Q \end{Bmatrix}=n_{Qa}n_{abx} \times\begin{cases}(-1)^{a+x}n_{lx}n_{cb}^{-1}[c]^{-1} & \text{for } c=l+Q \\ (-1)^{a+b}n_{cb}n_{lx}^{-1}[l]^{-1} & \text{for } c=l-Q \, . \end{cases} \tag{A13}$$

When $Q=1$ this equation can be applied to the case $c=c'$, but for the interference case $c\neq c'$ we have not found a simple formula.

Assuming that no equation between "normal" physical quantities contains square roots these procedures provide a check on our deviations. Furthermore, the equations become easier to handle. Nonphysical quantities may still contain square roots, e.g., $C_1^1=-(1/\sqrt{2})(x+iy)$ and 3-j symbols that are not of the form of Eq. (A12). This is because the m components other than zero are "artificial" unitary linear combinations. A physical quantity will always contain, e.g., $x=-(C_1^1+C_{-1}^1)/\sqrt{2}$. Likewise 3-$j$ symbols will always be combined in such a way as to give well-behaved numbers when multiplied by Δ factors, as in Eq. (8).

The transformation from Eq. (1) to Eq. (2) is the most simple form of recoupling of six moments.[37] It reconnects six outgoing lines, pairing the "natural" partners (l,l), (c,c'), and (Q,Q), such as to give a multipole expansion. The procedure essentially starts using the orthogonality relation for 3-j symbols

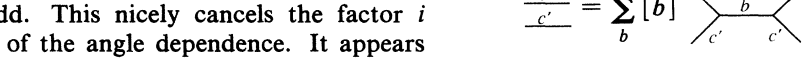

$$\sum_b [b] \, . \tag{A14}$$

Three of these steps produce

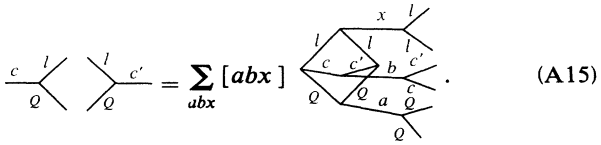

$$\sum_{abx}[abx] \, . \tag{A15}$$

Application of theorem 3 of Yutsis, Levinson, and Vanagas (YLV3) (Refs. 35 and 36) then cuts the lines a, b, and x and connects the ends in both parts

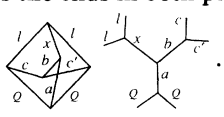

$$\sum_{abx}[abx] \, . \tag{A16}$$

This result is slightly rewritten in Eqs. (2) and (18).

[1]G. van der Laan, B. T. Thole, G. A. Sawatzky, J. B. Goedkoop, J. C. Fuggle, J. M. Esteva, R. C. Karnatak, J. P. Remeika, and H. A. Dabkowska, Phys. Rev. B **34**, 6529 (1986).
[2]G. van der Laan, Phys. Rev. Lett. **66**, 2527 (1991); J. Phys.: Condens. Matter **3**, 1015 (1991).
[3]B. T. Thole and G. van der Laan, Phys. Rev. B **44**, 12 424 (1991).
[4]G. van der Laan and B. T. Thole, Phys. Rev. B **48**, 210 (1993).
[5]C. N. Yang, Phys. Rev. **74**, 764 (1948).
[6]H. A. Bethe and E. E. Salpeter, *Quantum Mechanics of One and Two Electron Atoms* (Academic, New York, 1957), p. 308.
[7]J. Cooper and R. N. Zare, J. Chem. Phys. **48**, 942 (1968).
[8]V. L. Jacobs, J. Phys. B **5**, 2257 (1972).
[9]H. Klar and H. Kleinpoppen, J. Phys. B **15**, 933 (1982).
[10]U. Fano and G. Racah, *Irreducible Tensorial Sets* (Academic, New York, 1959).
[11]See, e.g., L. C. Biedenharn, G. B. Arfken, and M. E. Rose, Phys. Rev. **83**, 586 (1951); G. B. Arfken, M. E. Rose, and L. C. Biedenharn, *ibid.* **86**, 761 (1952); L. C. Biedenharn, Rev. Mod. Phys. **25**, 729 (1953); L. C. Biedenharn, in *Nuclear Spectroscopy,* edited by F. Ajzenberg-Selove (Academic, New York, 1969), Part B.
[12]U. Fano and D. Dill, Phys. Rev. A **6**, 185 (1972).
[13]H. Klar, J. Phys. B **13**, 3117 (1980).
[14]N. M. Kabachnik and I. P. Sazhina, J. Phys. B **9**, 1681 (1976).
[15]Dan Dill, Phys. Rev. A **6**, 160 (1972).
[16]B. Ritchie, Phys. Rev. A **13**, 1411 (1976).
[17]N. A. Cherepkov, Chem. Phys. Lett. **87**, 344 (1982).
[18]R. L. Dubs, S. N. Dixit, and V. McKoy, Phys. Rev. Lett. **54**, 1249 (1985).
[19]G. Schönhense, Phys. Scr. **T31**, 255 (1990).
[20]M. Pahler, C. Lorentz, E. v. Raven, J. Rüder, B. Sonntag, S. Baier, B. R. Müller, M. Schulze, H. Staiger, P. Zimmerman, and N. M. Kabachnik, Phys. Rev. Lett. **68**, 2285 (1992).
[21]U. Fano and J. H. Macek, Rev. Mod. Phys. **45**, 553 (1973).
[22]D. A. Case, G. M. McClelland, and D. R. Herschbach, Mol. Phys. **35**, 541 (1978); M. P. Docker, Chem. Phys. **125**, 185 (1988).
[23]C. H. Greene and R. N. Zare, J. Chem. Phys. **78**, 6741 (1983).
[24]R. N. Dixon, J. Chem. Phys. **85**, 1866 (1986); P. L. Houston, Phys. Chem. **91**, 5388 (1987).
[25]M. P. Docker, Chem. Phys. **135**, 405 (1989).
[26]Ch. Roth, F. U. Hillebrecht, H. B. Rose, and E. Kisker, Phys. Rev. Lett. **70**, 3479 (1993).
[27]C. M. Lee, Phys. Rev. A **10**, 1598 (1974).
[28]L. Baumgarten, C. M. Schneider, H. Petersen, F. Schäfers, and J. Kirschner, Phys. Rev. Lett. **65**, 492 (1990).
[29]C. M. Schneider, D. Venus, and J. Kirschner, Phys. Rev. B **45**, 5041 (1992).
[30]D. Venus, C. M. Schneider, C. Boeglin, and J. Kirschner, J. Phys.: Condens. Matter **5**, 1239 (1993).
[31]A. Liebsch, Phys. Rev. B **13**, 544 (1976).
[32]C. S. Fadley, in *Synchrotron Radiation Research,* edited by R. Z. Bachrach (Plenum, New York, 1992), Vol. 1, p. 421.
[33]J. J. Barton, Phys. Rev. Lett. **61**, 1356 (1988).
[34]B. P. Tonner, Z. L. Han, G. P. Harp, and D. K. Saldin, Phys. Rev. B **43**, 14 423 (1991).
[35]D. M. Brink and G. R. Satchler, *Angular Momentum* (Clarendon, Oxford, 1962), Chap. 7.
[36]A. P. Yutsis, I. B. Levinson, and V. V. Vanagas, *Mathematical Apparatus of the Theory of Angular Momentum* (Israel Program for Scientific Translation, Jerusalem, 1962).
[37]D. A. Varshalovich, A. N. Moskalev, and V. K. Khersonskii, *Quantum Theory of Angular Momentum* (World Scientific, Singapore, 1988), p. 438.
[38]D. A. Varshalovich, A. N. Moskalev, and V. K. Khersonskii, *Quantum Theory of Angular Momentum* (Ref. 37), Sec. 5.16.
[39]P. Carra, B. T. Thole, M. Altarelli, and X. Wang, Phys. Rev. Lett. **70**, 694 (1993).
[40]R. D. Cowan, *The Theory of Atomic Structure and Spectra* (University of California Press, Berkeley, 1981).
[41]B. T. Thole, X. D. Wang, B. N. Harmon, Dongqi Li, and P. A. Dowben, Phys. Rev. B **47**, 9098 (1993).
[42]P. H. Butler, *Point Group Symmetry, Applications, Methods and Tables* (Plenum, New York, 1981), Chap. 16.
[43]S. M. Goldberg, C. S. Fadley, and S. Kono, J. Electron Spectrosc. Relat. Phenom. **21**, 285 (1981).
[44]L. C. Biedenharn and J. D. Louck, *Angular Momentum in Quantum Physics,* Encyclopedia of Mathematics Vol. 8 (Addison-Wesley, Reading, MA, 1981), Sec. 6.17.
[45]D. A. Varshalovich, A. N. Moskalev, and V. K. Khersonskii, *Quantum Theory of Angular Momentum* (Ref. 37), Sec. 5.16.2.
[46]G. van der Laan, M. A. Hoyland, M. Surman, C. F. J. Flipse, and B. T. Thole, Phys. Rev. Lett. **69**, 3827 (1992).
[47]P. A. Dowben, D. LaGraffe, Dongqi Li, A. Miller, and Ling Zhang, Phys. Rev. B **43**, 3171 (1991).
[48]R. I. R. Blyth, A. J. Patchett, S. S. Dhesi, R. Cosso, and S. D. Barrett, J. Phys. Condens. Matter **3**, S287 (1991).
[49]K. Starke, E. Navas, L. Baumgarten, and G. Kaindl, Phys. Rev. B **48**, 1329 (1993).
[50]J. Bansmann, Ch. Ostertag, G. Schönhense, F. Fegel, C. Westphal, M. Getzlaff, F. Schäfers, and H. Petersen, Phys. Rev. B **46**, 13 496 (1992).
[51]S. M. Goldberg, C. S. Fadley, and S. Kono, Solid State Commun. **28**, 459 (1978).
[52]D. A. Varshalovich, A. N. Moskalev, and V. K. Khersonskii, *Quantum Theory of Angular Momentum* (Ref. 37), Sec. 8.5.2, Eq. (42).
[53]See, e.g., D. A. Varshalovich, A. N. Moskalev, and V. K. Khersonskii, *Quantum Theory of Angular Momentum* (Ref. 37), Sec. 10.2.1, Eq. (1); or S. M. Goldberg, C. S. Fadley, and S. Kono (Ref. 43), Eq. (3.326).
[54]This can be derived from Eq. (9) in D. A. Varshalovich, A. N. Moskalev, and V. K. Khersonskii, *Quantum Theory of Angular Momentum* (Ref. 37), Sec. 10.8.3.
[55]B. T. Thole, G. van der Laan, J. C. Fuggle, G. A. Sawatzky, R. C. Karnatak, and J. M. Esteva, Phys. Rev. B **32**, 5107 (1985).

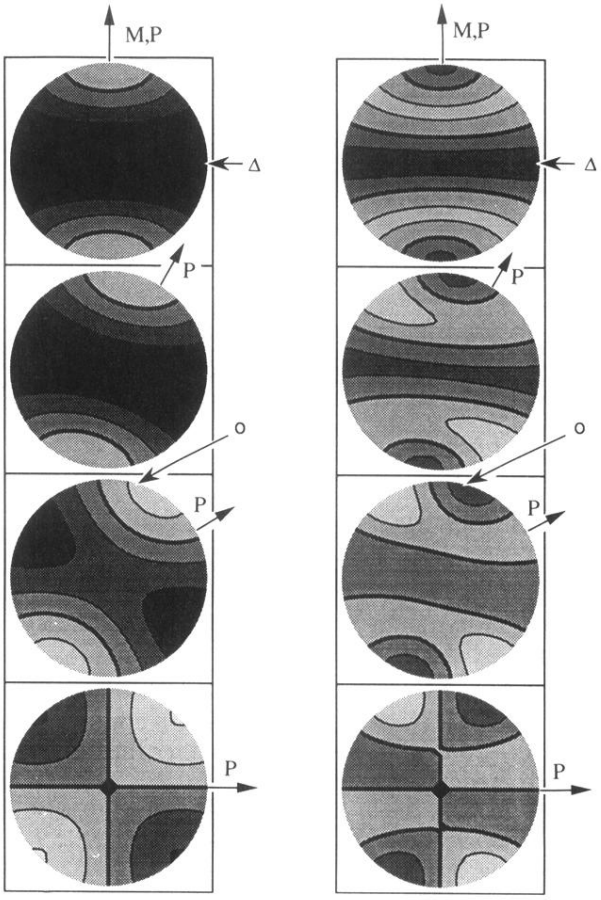

a) $-\frac{3}{7} U^{101} + \frac{30}{49} U^{121}$ b) $\frac{10}{49} U^{123} - \frac{24}{49} U^{143}$

FIG. 6. Angular distribution of the coefficients for (a) I^1 and (b) I^3 in Eq. (79). The plots show the emission intensity from a viewpoint perpendicular to the **P**,**M** plane. In the four plots **M** is always in the vertical direction pointing upward while **P** is at 0, 30, 60, and 90° with **M**. The center of the circle gives the intensity in the direction perpendicular to the **P**, **M** plane. The radius of a plotted point is its polar angle with this direction. Thus the boundary of the circle gives the emission in **P**,**M** plane. The contours have intervals of 0.2, where the thick lines are the contours of zero intensity. Dark (light) grey denotes negative (positive) intensity. The approximate geometry used by Starke *et al.* (Ref. 49) is indicated by △. A geometry suitable for measuring I^3 is indicated by ○.